NIH Public Access
Author Manuscript
DNA Repair (Amst). Author manuscript; available in PMC 2010 June 4.

Published in final edited form as:
DNA Repair (Amst). 2009 June 4; 8(6): 704–719. doi:10.1016/j.dnarep.2009.01.021.

Novel DNA mismatch repair activity involving YB-1 in human mitochondria

Nadja C. de Souza-Pinto[1,*], **Penelope A. Mason**[1], **Kazunari Hashiguchi**[1,@], **Lior Weissman**[1], **Jingyan Tian**[1], **David Guay**[2], **Michel Lebel**[2], **Tinna V. Stevnsner**[3], **Lene Juel Rasmussen**[4], and **Vilhelm A. Bohr**[1,§]

1 *Laboratory of Molecular Gerontology, NIA-IRP, National Institutes of Health, Baltimore, MD, USA*

2 *Centre de recherche en cancérologie, Département Hôpital Hôtel-Dieu de Québec, Quebec, Canada*

3 *Danish Centre for Molecular Gerontology, Department of Molecular Biology, Aarhus University, Denmark*

4 *Department of Science, Systems and Models, Roskilde University, Denmark*

Abstract

Maintenance of the mitochondrial genome (mtDNA) is essential for proper cellular function. The accumulation of damage and mutations in the mtDNA leads to diseases, cancer, and aging. Mammalian mitochondria have proficient base excision repair, but the existence of other DNA repair pathways is still unclear. Deficiencies in DNA mismatch repair (MMR), which corrects base mismatches and small loops, are associated with DNA microsatellite instability, accumulation of mutations, and cancer. MMR proteins have been identified in yeast and coral mitochondria; however, MMR proteins and function have not yet been detected in human mitochondria. Here we show that human mitochondria have a robust mismatch-repair activity, which is distinct from nuclear MMR. Key nuclear MMR factors were not detected in mitochondria, and similar mismatch-binding activity was observed in mitochondrial extracts from cells lacking MSH2, suggesting distinctive pathways for nuclear and mitochondrial MMR. We identified the repair factor YB-1 as a key candidate for a mitochondrial mismatch-binding protein. This protein localizes to mitochondria in human cells, and contributes significantly to the mismatch-binding and mismatch-repair activity detected in HeLa mitochondrial extracts, which are significantly decreased when the intracellular levels of YB-1 are diminished. Moreover, YB-1 depletion in cells increases mitochondrial DNA mutagenesis. Our results show that human mitochondria contain a functional MMR repair pathway in which YB-1 participates, likely in the mismatch binding and recognition steps.

Keywords

Base mismatches; Microsatellite instability; Mismatch repair; Mitochondria; Mitochondrial DNA; YB-1

§Corresponding author: Dr. Vilhelm A. Bohr, MD, PhD, DSci, Laboratory of Molecular Gerontology, National Institute on Aging/ Intramural Research Program, National Institutes of Health, 5600 Nathan Shock Drive, Baltimore, MD 21224, Tel.: 410-558-6288, Fax: 410-558-8157, E-mail: E-mail: vbohr@nih.gov.
*Current address: Dept. of Biochemistry, Institute of Chemistry, University of São Paulo, Brazil
@Current address: Laboratory of Radiation Biology, Graduate School of Science, Kyoto University, Japan

The authors declare no conflict of interest

Publisher's Disclaimer: This is a PDF file of an unedited manuscript that has been accepted for publication. As a service to our customers we are providing this early version of the manuscript. The manuscript will undergo copyediting, typesetting, and review of the resulting proof before it is published in its final citable form. Please note that during the production process errors may be discovered which could affect the content, and all legal disclaimers that apply to the journal pertain.

NIH-PA Author Manuscript
NIH-PA Author Manuscript
NIH-PA Author Manuscript

NIH-PA Author Manuscript

NIH-PA Author Manuscript

NIH-PA Author Manuscript

INTRODUCTION

The human mitochondrial genome (mtDNA) is a small, circular, highly-coding molecule (Anderson *et al.*, 1981), making mtDNA mutations more likely to be deleterious than nuclear ones (Larsson and Clayton, 1995;Nagley and Wei, 1998). Due to its proximity to the electron transport chain, the mtDNA is exposed to high levels of reactive oxygen species, increasing the risk of oxidative DNA damage (Richter *et al.*, 1988;Yakes and Van, 1997;Ben Yehuda *et al.*, 2000). Until recently, mammalian mitochondria were not thought to possess any DNA repair activities (Clayton *et al.*, 1974), however, it is now clear that mitochondria are proficient in DNA repair of certain types of DNA lesions, particularly those repaired by the base excision repair (BER) pathway, which removes oxidative and alkylating damage.

Whilst all the core enzymatic components of the BER pathway have been found in mammalian mitochondria (Dianov *et al.*, 2001;Mandavilli *et al.*, 2002;Kang and Hamasaki, 2002;Bohr, 2002), the existence of other DNA repair pathways in this organelle is unclear, owing partially to the technical challenges inherent in studying mtDNA metabolism, particularly in humans. While there is no evidence for the existence of nucleotide excision repair (NER), the presence of recombinational repair (Thyagarajan *et al.*, 1996;Kajander *et al.*, 2001) and end-joining (Lakshmipathy and Campbell, 1999) in mammals (including humans) have been suggested.

DNA microsatellite instability (MSI) is a hallmark of several types of cancer (Fang and Modrich, 1993;Fliss *et al.*, 2000;Bianchi *et al.*, 2001;Tan *et al.*, 2002b;Kumimoto *et al.*, 2004;Kose *et al.*, 2005). Both nuclear and mitochondrial MSI have been linked to colorectal (Habano *et al.*, 1998;Lievre *et al.*, 2005) and gastric (Habano *et al.*, 2000b) carcinomas. Interestingly, while one study (Habano *et al.*, 2000a) suggests a positive correlation between nuclear and mitochondrial MSI, several others indicate that these two events often do not correlate (Alazzouzi *et al.*, 2003;Fang *et al.*, 2004;Kose *et al.*, 2006), suggesting that the disruption of distinct pathways is responsible for their formation. Nuclear MSI has been proposed to result from DNA slippage and mispairing in repetitive DNA sequences during DNA replication. DNA mismatch repair (MMR) suppresses MSI (Harfe and Jinks-Robertson, 2000) through its role in repairing DNA mismatches and small loops. MMR deficiency increases cellular mutation rates and is associated with cancer susceptibility. Most notably, human hereditary non-polyposis colon cancer (HNPCC) is linked to mutations in nuclear MMR proteins (Buermeyer *et al.*, 1999), with nuclear MSI being a hallmark of this disease.

In addition to microsatellite instability (Tan *et al.*, 2002a) (Habano *et al.*, 1999), various other mutations (Polyak *et al.*, 1998) have been detected in mtDNA from cancer patients. Mismatch repair proteins have not yet been identified in mammalian mitochondria, however, a *bone fide* mismatch repair protein localizes to yeast mitochondria: a MutS homologue called MSH1 that when disrupted causes a severe mtDNA instability phenotype (Reenan and Kolodner, 1992;Chi and Kolodner, 1994a;Chi and Kolodner, 1994b). In addition, the mitochondrial DNA from at least one coral species (*Sarcophyton glaucum*) encodes for a MMR protein, an MSH2 homologue (Pont-Kingdon *et al.*, 1998). Further, *in vitro* studies have demonstrated a MMR activity in mitochondrial lysates from rat liver (Mason *et al.*, 2003), although none of the enzymatic components were identified. Mammalian mitochondria also repair cisplatin cross-links (LeDoux *et al.*, 1992), which, in the nucleus, are recognized by MMR as well as NER proteins (Fink *et al.*, 1996;Vaisman *et al.*, 1998;Claij and te, 2004), even though MMR has not been implicated in the repair of cisplatin-induced DNA lesions (Sansom *et al.*, 2001). The results presented above suggest that there might be a functional MMR pathway in mitochondria, which, when disrupted may lead to MSI and mtDNA instability.

In this study we followed up on the observation by Mason and colleagues (Mason *et al.*, 2003) that rat liver mitochondria can support MMR. We aimed to identify MMR in human

NIH-PA Author Manuscript

NIH-PA Author Manuscript

NIH-PA Author Manuscript

mitochondria. We identified a robust *in vitro* mismatch repair activity in highly purified mitochondrial extracts that was inhibited by a DNA polymerase γ inhibitor. We also characterized a mismatch-binding activity that was not dependent upon classic nuclear MMR factors. The mismatch-binding activity co-purified with YB-1, a multifunctional protein (Kohno *et al.*, 2003), known to be implicated in the nuclear BER pathway (Das *et al.*, 2007), and which has been shown to melt mismatch- and cisplatin-containing DNA duplexes in vitro (Gaudreault *et al.*, 2004). Mitochondrial extracts depleted of YB-1 showed a significantly decreased mismatch-binding and repair activity; while decreased expression of YB-1 resulted in lower cellular respiration, suggesting mitochondrial dysfunction. More importantly, cells depleted of YB-1 showed increased mtDNA mutagenesis, implicating this protein in mutation avoidance. Therefore, we propose the existence of a novel human mitochondrial MMR pathway, which includes YB-1 as one of its participants.

MATERIALS and METHODS

Chemicals and enzymes

Where not stated, all reagents were of the highest grade obtainable. Cell culture media and supplements were from Invitrogen, including Prolong Gold mounting medium with DAPI. Purified hMutSα protein (Acharya *et al.*, 1996) was a kind gift from Dr. Teresa Wilson (University of Maryland). Antibodies to human MSH2 (SC-494), MSH3 (SC-5686), MLH1 (SC-11442), and GRB2 (SC-255) were from Santa Cruz. YB-1 (ab 12148) and MSH6 (ab 10896) antibodies were from Abcam. Antiserum to polymerase β (clone 61) was from Trevigen, and Lamin B was from Novocastra; Cytochrome c oxidase subunit IV (20E8) was from Molecular Probes. Top1 (2012-2) antibody was from Topogen and anti-TDG (SM1403P) was from Acris GmBH. AlexaFluor 488-conjugated secondary antibodies (A-11034 and A-21121) were from Invitrogen. Oligonucleotides were from Midland or IDT; all sequences are presented in Table 1. SiRNA duplices against YB-1 (NSEP1, #16708A: ID 5109, 5201, and 115543) were from Ambion. Non-targeting negative siRNA (D-001210-02) and positive control siRNA to Lamin A/C (D-001050-01) were from Dharmacon. FuGene 6 was from Roche.

Cell culture

HEC59 and HEC59/2–4 cell lines were kind gifts from Dr. Timothy J. Kinsella (University Hospitals of Cleveland) and grown as described previously (Morisawa, 1987;Umar *et al.*, 1994b;Boyer *et al.*, 1995;Umar *et al.*, 1997). Human lymphoblastoid GM1310 cells were grown in RPMI 1640 supplemented with 2 mM L-glutamine, 10% fetal bovine serum and antibiotics. HHUA, HHUA+chr2 and HHUA+chr5 cells were kind gifts from Dr. Tom Kunkel/ Alan Clark, (NIEHS/NIH) and grown in DMEM/F12 +glutamax (1:1), 10% heat inactivated and dialyzed fetal bovine serum. For HHUA+chr2 and HHUA+chr5 400 μg/ml Geneticin was included in the media. All cell lines were maintained at 37°C, in a 95% air/5% CO_2 atmosphere. Fresh HeLa S3 cell pellets were purchased from the National Cell Culture Center (Minneapolis, MN).

Preparation of whole cell and mitochondrial extracts

At 80% confluence, monolayer and suspension cultures were harvested, washed twice with PBS and immediately used to prepare whole cell and mitochondrial extracts, unless stated. Intact mitochondria were purified by differential centrifugation followed by Percoll gradient; mitochondrial extracts were prepared as described previously (Croteau *et al.*, 1997). Mitoplasts were prepared from mitochondria essentially as in (Schnaitman and Greenawalt, 1968) using digitonin and pelleting at 12000×g, and were Proteinase K-treated and washed 5x before sonication. Whole cell and nuclear extracts were prepared as in (Dignam *et al.*, 1983). Protein concentration was determined using a Bio-Rad protein assay kit with bovine serum albumin

NIH-PA Author Manuscript

NIH-PA Author Manuscript

NIH-PA Author Manuscript

as a standard, according to the manufacturer's instructions. Purity of the mitochondrial extracts was analyzed by Western blot using anti-DNA polymerase β or anti-Lamin B, and anti-cytochrome c oxidase subunit IV antibodies as nuclear/cytosolic and mitochondrial marker proteins, respectively. For these and subsequent blots, unless otherwise stated the standard amount of protein per well was 30 μg total protein.

Electrophoretic mobility shift assays (EMSA)

Ten nM of ^{32}P-labeled oligonucleotides were mixed with 15 μg total mitochondrial or mitoplast extracts in 10 mM Tris-HCl pH 7.4, 20 mM NaCl, 25 mM KCl, 0.5 mM EDTA, 0.5 mM dithiothreitol, 10 ng/μl BSA, 2 ng/μl poly[dI-dC] and 5% glycerol as standard. After binding (10 μl total, 30 min 4°C), reactions were separated (4°C/200 V/2 hr) on a 5% polyacrylamide (19:1) gel in 1xTBE and 5% glycerol. Analysis used PhosphoImager and ImageQuant software quantification (GE Healthcare). Purified YB-1 EMSA was performed essentially as described in (Machwe *et al.*, 2002). For cross-linking (supplemental Fig 2), substrate contained two bromodeoxyuridine (BrdU) residues to allow for covalent binding (Table 1). After binding, reactions were UV-irradiated for 1~5 min (UV Stratalinker, Stratagene). Half-samples were loaded onto native PAGE for EMSA and the rest were heat-denatured (95°C, 5 min) and analyzed on 12% SDS-PAGE.

Purification of HeLa mitochondria mismatch-binding proteins

Mitoplasts were made from 50 litres of fresh log phase HeLa cells. After disruption of the inner membrane with sonication, the resulting lysate was purity-tested and loaded onto a 5 ml DEAE anion-exchange column (GE Healthcare) in Buffer A (25 mM HEPES-KOH pH 7.9, 2 mM DTT, 1 mM EDTA, 150 mM KCl, 0.01% NP-40, 0.1% PMSF). Active fractions, identified using EMSA (Fig S2 C), were pooled together, concentrated via Centricon 3 (Millipore) and equilibrated in Buffer B (Buffer A with 300 mM KCl). The resulting fractions of interest were loaded separately onto Superose-6 HR gel filtration columns, and the peaks of interest were collected for further analysis. For both columns, 15 μl (3%) of each 0.5ml fraction was subjected to EMSA (+1 IDL duplex), otherwise EMSA conditions were as above.

Affinity purification

Fifty pmol +1 IDL substrate conjugated to biotin, and the corresponding homoduplex, were incubated (1h RT) with 100 μl of pre-cleaned and blocked MyOne streptavidin-conjugated Dynabeads (Dynal) in 25 mM HEPES-NaOH pH7.8, 1 mM EDTA, 1 mM DTT, 10% glycerol, 0.1 M NaCl. The bead-oligo conjugate was recovered, washed three times with 1x PBS to remove excess nucleic acid, then incubated with 4 mg of the FPLC-enriched mitochondrial lysate (1h at 4°C). After washing again 5x, putative bound proteins were recovered by step-wise salt elution (1 and 2 M NaCl, each 1h 4°C), followed by incubation at 95°C/3 min. in SDS-PAGE buffer. Aliquots of each elution were separated by SDS-PAGE and differentially enriched species removed for Mass Spectrometry analysis (NIA Mass Spectrometry service).

Immunocytochemistry

HeLa cells, cultured on chambered slides to approx. 70% confluence, were incubated with 50 nM MitoTracker Red (Molecular Probes) for 30 min. Excess dye was removed by washing with fresh medium for 1–5 h and the cells were fixed as described in (Indig *et al.*, 1997). When indicated, 50 μM thymidine was added immediately after the MitoTracker loading. Nuclei were stained using mounting medium containing DAPI as per the manufacturer's instructions, and the desired proteins visualized using the appropriate primary antibody and AlexaFluor 488-conjugated secondary antibody. GFP-tagged YB-1 was transiently transfected into HeLa cells using FuGene 6 as per the manufacturer's specifications, and the cells imaged live 25 h later, after MitoTracker and thymidine treatment. Confocal imagery used a Nikon Eclipse

NIH-PA Author Manuscript

NIH-PA Author Manuscript

NIH-PA Author Manuscript

TE2000E with a 100x/1.30 oil plan fluor objective. Co-localization was calculated using the Improvison's Volocity software to give a Pearson's correlation co-efficient (where 0 indicates random overlap and 1 perfect correlation); thresholds are given. Live imaging used a Zeiss Axiovert 200M microscope and 63x/1.2 oil objective. For each experiment, at least ten cells from twenty-five different fields were visualized. Experiments were repeated three times independently

SiRNA knockdown

HeLa cells were subjected to siRNA knockdown of YB-1 using DharmaFECT 1 transfection reagent, following the Dharmacon's HeLa cell protocol, but using 50 nM siRNA. The siRNA experiments utilised a mix of three siRNA's that targeted exons 2, 3 and 5 of YB-1, respectively. Knockdown was confirmed via YB-1 Western analysis and quantified using ImageQuant software (GE HealthCare).

MMR assays

M13-based *in vitro* MMR assays, using a dG/dG3' M13 substrate, have been described elsewhere (Mason *et al*., 2003). Plaques were scored after at least 16 h incubation at 37°C and 4–8 h at 4°C. Aphidicolin was used at 120 μM, ethidium bromide at 40 μM, and purified GST-YB-1 or GST at 4 nM, when indicated. Initial scoring was performed blind to test reproducibility of the results, and then repeated three times (twice with aphidicolin or ethidium bromide). Recovered samples for each independent experiment were electroporated twice (2 plates each) and the resulting plaque numbers added to give the scores for each experiment. Two-tailed *T*-test analyses were performed for statistical significance, assuming a normal distribution for both sample populations. Resulting *p*-values are given.

To validate the mismatch repair activities obtained from the plaque assay, extracts were also tested for their ability to repair a dG/T mismatch substrate that contained a single-stranded nick located 5′ to the unpaired bases. *In vitro* repair reactions containing 100 ng heteroduplex and 100 μg mitochondrial extract were carried out as described in (Wang and Hays, 2003). Briefly, the substrate was incubated with the extracts, transformed into MutS-deficient *E. coli* and DNA isolated from a number of colonies. Repair was assessed by restriction digest; repaired heteroduplex shows three species (865 bp, 793 bp, and 346 bp) while unrepaired heteroduplex (wild-type and mutant plasmid) shows four species (1139 bp, 865 bp, 793 bp, and 346 bp) after digestion.

Oxygen consumption measurement

Cellular oxygen consumption was measured using the BD Oxygen Biosensor 96-well plates (BD Biosciences), according to the manufacturer's instructions. Briefly, HeLa cells were transfected with 50 nM YB-1 siRNA every 5 days, for 15 days, in the presence of thymidine as described above. After 72 h recovery in absence of thymidine, cells were plated into a pre-scanned Biosensor plate at 1×10^5 cells/well, in sextuplicate. Cells were equilibrated for 5 h in the incubator and the fluorescence (485nm ex./620nm em) was read. One hundred mM Na_2SO_3 was used as a zero oxygen control and medium alone was used for measuring ambient oxygen. Fluorescence readings for each well were normalized to the pre-scan of the dry plate and normalized to the average Na_2SO_3 reading, as suggested by the manufacturer.

Chloramphenicol resistance assay

Chloramphenicol (CAP)-resistance was measured as a measurement of mtDNA mutagenesis. For the selection assay, HeLa cells were seeded onto 6-well dishes at 500 cells/well, and 24 h later the growth medium was replaced with medium containing 300 μg/ml CAP. For measurement of plate efficiency, wells subjected to the same experimental conditions were

NIH-PA Author Manuscript

NIH-PA Author Manuscript

NIH-PA Author Manuscript

incubated in absence of CAP. The cultures were maintained until colonies visible to the naked eye were formed; the colonies were then fixed with methanol and stained with 0.5% methylene blue. The number of colonies per well was measured using a Typhoon (GE Healthcare), with the colony-counting mode. The relative survival rate was calculated by dividing the average number of colonies in presence of CAP by the average number of colonies in absence of CAP for each experimental condition. For the Antimycin A treatment (AA), HeLa cells, grown to 40–50% confluence, were exposed to increasing concentrations of AA in growth medium, for 72 h. The cells were then replated into 6-well dishes at 500 cells/well and selected for CAP-resistance as described above. For the YB-1 knockdown experiments, HeLa cells were subjected to siRNA knockdown following the Dharmacon-recommend protocol for HeLa cells, using siRNAs target to exon 2 (siRNA1) and 3 (siRNA2). Seventy-two h after the transfection the cells were replated into 6-well dishes at 500 cells/well and selected for CAP-resistance, as described above.

RESULTS

HeLa mitoplast lysates can repair a mismatched circular substrate

Mitochondria were isolated from HeLa and GM1310 cells and further purified by removing the outer membrane with digitonin and incubation with Proteinase K to digest any non-mitochondrial protein remaining in the sample. After washing, the mitoplast fractions were sonicated to disrupt the inner membrane. Mitochondrial purity was tested via Western Blot (WB) using antisera to Polymerase β, Lamin B, and Growth factor receptor-bound protein 2 (GRB2) as nuclear/cytosolic markers, and COX IV as mitochondrial markers, respectively (Fig. 1A shows representative blots). While all 3 marker proteins were readily detected in whole cell (WCE) and nuclear extracts (N), no signal for pol β or Lamin B (two nuclear proteins) was detected in mitochondrial extracts (ME). For the GRB2 cytosolic marker, a small band was detected in the mitochondrial fraction only when we used 4 times more mitochondrial protein (60 μg ME and 15 μg WCE). After normalization of the WB bands to loading, the relative contamination of the mitochondrial extracts with non-mitochondrial markers was estimated to be between 1.4 to 4%, indicating a high degree of purity.

In order to determine whether human mitochondria possess active mismatch repair we next assayed these extracts for DNA mismatch repair activity *in vitro* using a well characterized M13-based MMR assay (Thomas *et al.*, 1991). This assay measures mutagenesis in an M13 β-galactosidase gene after incubating a heteroduplex plasmid containing the gene with one mismatch with the extract of interest, thus testing the repair capabilities of cellular lysates. The analysis utilizes phage readout and blue/white selection to calculate the *in vitro* repair percentages sustained by specific cell lysates. This is expressed as 1 – the ratio of the percentages of mixed burst (unrepaired) plaques obtained from treated and untreated 'mock' (no addition of lysate) substrates. We used a dG/dG3′ mismatched substrate since dG/dG mismatches are not substrates for any known mitochondrial DNA glycosylases.

The mitoplast lysates were tested for DNA repair activity along with HeLa WCE as the positive, repair-proficient control, and LoVo cytosolic lysate as negative control (Fig. 1B). The LoVo cell line is derived from an HNPCC individual, and is deficient in key proteins involved in nuclear MMR (Liu *et al.*, 1995); lysates derived from this line showed no significant repair activity (4.5%) (lacking nuclear MMR activity). HeLa mitochondrial extracts showed clear mismatch repair activity (33%), which is significantly higher than the negative control (p = 0.0062). For comparison, similar amounts of HeLa WCE (MMR proficient) showed repair activity of about 60 %.

Mismatch repair requires the activity of a DNA polymerase to incorporate the correct nucleotide in place of the removed mismatched one. DNA polymerase γ (Pol γ) is the only

NIH-PA Author Manuscript

NIH-PA Author Manuscript

NIH-PA Author Manuscript

polymerase identified in mitochondria so far. It participates in both DNA replication and base excision repair (Copeland and Longley, 2003). Thus, we tested whether pol γ participated in this newly identified MMR pathway by performing *in vitro* DNA repair assays in the presence of 40 μM ethidium bromide, which reduces DNA pol γ activity at least 80% *in vitro* (Tarrago-Litvak *et al.*, 1978) (Fig. 1C). Ethidium bromide significantly reduced MMR activity in HeLa mitochondrial extracts, from 34 ± 3.9% to 11 ± 0.2 (see Table 5 for plaque counts), suggesting that pol γ participates in mitochondrial MMR. Some reduction in MMR activity was also observed in the HeLa WCE and LoVo extracts (17% for the HeLa WCE and 78% for LoVo lysates), possibly suggesting that mitochondria may contribute to whole cell extracts mismatch repair activity in both samples.

Nuclear mismatch-binding proteins do not co-localize to mitochondria

Nuclear mismatch repair homologues have been reported in mitochondria from yeast and coral, but studies have disagreed as to whether hMSH2 and hMLH1 are found in mitochondria in human cells (Mason *et al.*, 2003;Bannikova *et al.*, 2005). In order to determine whether the MMR activity we detected in human mitochondria was due to mitochondria-localized homologues of nuclear MMR proteins we investigated whether nuclear MMR proteins localize to HeLa mitochondria using immunocytochemistry analysis with antibodies to monitor whether hMSH3, hMSH6, and hMLH1 localize in the mitochondria as well as in the nuclei of HeLa cells. MitoTracker Red (CMX Ros) was used to identify this organelle. In order to increase the frequency of DNA mismatches in the mtDNA, and thus the likelihood of MMR proteins relocating to mitochondria, cells were grown in the presence or absence of thymidine, which alters intracellular nucleoside pools and increases mispairing frequency during mtDNA replication (Song *et al.*, 2003).

Fig. 2 shows confocal microscopy at 100× magnification of thymidine-treated HeLa cells. The red color indicates mitochondria (Mitotracker Red) (MT) and the blue shows the nucleus (DAPI staining). All three nuclear MMR proteins analysed, MSH3, MSH6, and MLH1, showed almost exclusive nuclear localization. No co-localization with mitochondria was detected for any of these proteins (see the enlarged ‘Merge’ images for detail) in the thymidine treated as well as in those not exposed to excess thymidine (not shown).

DNA mismatch-binding activity in lysates of human mitochondria

Mismatch repair initiates by the mismatch recognition and binding by specific protein complexes. Thus, we reasoned that human mitochondria contain mismatch binding protein(s). In order to identify a mismatch binding activity in human mitochondria we used 30-mer oligonucleotide duplexes containing either single-base mismatches or insertion/deletion loops (sequences and structures are shown in Table 1). Guanine mismatches were selected because dG/T and dG/dA are the most stable DNA mismatches (Marra and Schar, 1999) and a dG/dG mismatch is not a substrate for any known mitochondrial glycosylase, such as OGG1 or MYH glycosylases.

Mismatch-binding was detected using EMSA assay (see Fig. 3A, binding species are labelled a–c). HeLa mitochondrial extracts showed significant binding of substrates containing dG/dG, dG/dA and dG/T mismatches (Fig. 3A, lanes 2–4) but not of a control, dG:dC homoduplex (lane 5). The binding to the dG/dG substrate was disrupted upon boiling (95°C for 5 min; lane 6), suggesting that the complex is not covalently bound and that the binding activity probably includes protein components. This observation distinguishes the mismatch-binding species from DNA topoisomerase I (Top1), which nicks DNA mismatches and forms a heat-insensitive 3′-covalent complex at the cleavage site (Wang, 2002). Moreover, a hTop1 antibody did not supershift any of the EMSA species (data not shown).

NIH-PA Author Manuscript

NIH-PA Author Manuscript

NIH-PA Author Manuscript

In addition to the DNA base mismatches we detected binding to 1 or 4 nucleotide loops (Fig. 3A, lanes 9 and 10), which are also classic substrates for nuclear MMR enzymes (Parsons *et al.*, 1993;Umar *et al.*, 1994a;Genschel *et al.*, 1998). Binding efficiency was slightly higher (but not significantly) for the looped substrates than for the dG/T mismatch (see Table 2 for quantification).

The mitochondrial mismatch binding activity was not competed out by single-stranded competitor DNA, but a significant reduction in binding was observed when double-stranded competitor DNA was used (Fig. 3B). A 20-fold excess of unlabeled dG:dC decreased binding of the labelled dG/dG substrate only partially (see Table 3 for quantifications). On the other hand, the 3 mismatched competitors significantly competed the binding to the labelled dG/dG mismatch. Since these experiments were done using mitochondrial extracts, and not purified proteins, we could not calculate affinity constants for the binding species. These results suggest that the binding is mismatch-specific.

Mitochondrial extracts from another human cell line, the normal human lymphoblastoid line GM1310, showed a similar mismatch binding profile to that of HeLa mitochondria (Fig. 3C) on a dG/dG substrate (lanes 1 and 3), which is also disrupted upon heating (lanes 2 and 4), suggesting that the mismatch binding activity, and MMR, are common features of human mitochondria.

In order to confirm that the binding species detected in the EMSA were of mitochondrial origin we compared the binding profile of whole cell extracts (WCE) against the mitochondrial (M) and mitoplast (MP) lysates (nuclear lysate showed an essentially similar binding pattern as the WCE) (Fig. 3D). Effective binding to the +1-nt loop substrate was detected in all 3 samples (lanes 2–4), but the profile for mitochondrial extracts was clearly distinct from that obtained with WCE. Because the native EMSA gels used in this experiment do not allow for an estimative of molecular weight of the binding species, we cannot assign the binding species in the WCE to any know nuclear MMR protein. However, the comparison between the migration patterns suggests that the protein species/complex involved in mismatch binding are different in these compartments, and it indicates that the activity detected in mitochondria is not due to nuclear contamination.

In the nucleus, base mismatches and loops are recognized by heteroduplexes containing the MutS homologue MSH2, MutSα and β. Even though this protein has not been detected either in rat liver mitochondria (Mason *et al.*, 2003) or in human mitochondria (Fig. 3E, top panel), MutS homologues have been identified in mitochondria from lower eukaryotes. We therefore tested whether MSH2 could participate in mismatch-binding in human mitochondria by comparing *hMsh2*-deficient HEC59 cells with HEC59/2–4 cells, complemented by the addition of chromosome 2, which carries the *Msh* gene, restoring MSH2 expression (Fig. 3E, top panel).

The EMSA assay using mitochondrial lysates obtained from these two cell lines was performed as before, with HeLa ME used as control (Fig. 3E, lanes 1 and 2). Mitochondrial extracts from both the MSH2-deficient (HEC59) and the MSH2-complemented (HEC59/2–4) cells showed binding activity to the dG/dG mismatch (lanes 3 and 5) stronger than that obtained with the HeLa mitochondrial extracts, which nonetheless migrated in the same position. Because we observed a higher unspecific binding (to the G:C homoduplex substrate) in mitochondrial extracts from these two cell lines, it is possible that the increased binding activity observed in these extracts is due in part, to such increased unspecific DNA binding activity. We also tested mitochondrial extracts from the MSH3 and −6 deficient cell line HHUA against chromosome 2 or 5 complemented HHUA cells (which restore MSH6 and MSH3 expression, respectively). Using the +1IDL substrate, which is a substrate for both MutSα and MutSβ, we found very small differences in the binding profile between extracts from cells deficient or proficient in

NIH-PA Author Manuscript

NIH-PA Author Manuscript

NIH-PA Author Manuscript

nuclear MMR proteins (Fig. S1). We observed a disappearance of the signal for the lower complex in both complemented cell lines. These differences, however, cannot be interpreted as evidence for an involvement of MSH6 or MSH3 in the mitochondrial mismatch-binding activity because, if that was the case, we should see an appearance of a bound complex in the complemented cell line rather than a disappearance.

The data presented here demonstrate that human mitochondria have a mismatch-specific DNA binding activity, which does not depend on MSH2. Together with the data obtained from the immunocytochemistry analyses (Fig. 2), these indicate that hMSH2, hMSH3, hMSH6, and hMLH1 are not present in human mitochondria, at least under the experimental conditions used in this study, and therefore do not contribute to the mitochondrial mismatch repair activity we show here.

Identification of mitochondrial mismatch-binding proteins in HeLa

In order to identify the mismatch binding species in HeLa mitochondrial extracts we first estimated the approximate molecular size of the binding species using mismatch substrates containing 3′-terminal BrdU residues (Table 1), which get covalently linked to the substrate DNA upon UV-irradiation. Mitochondrial extracts were incubated with the dG/dG-BrdU substrate and subsequently UV-irradiated for 1–5 min. (Fig. S2A and B). Three mismatch-specific species were detected as before (a-c), which sizes were estimated against molecular weight markers. Assuming the bound DNA contributes between 10 (if a single strand was cross-linked) or 20 kDa (if the duplex was cross-linked), molecular mass estimates after correction for the cross-linked DNA were calculated to be approximately 90–100, 60–70, and 30–40 kDa for species a–c, respectively.

To determine the identities of these mismatch-binding proteins we performed a large-scale purification of the mismatch-binding species from HeLa mitoplast lysate, as depicted in Fig. 4A. The lysates were fractionated as detailed in the Methods section (see also Fig. S2C). In order to recover the enriched binding proteins we used two distinct approaches, non-radioactive EMSA using the +1 IDL mismatched substrate or affinity purification using biotin-labelled mismatched DNA (Fig. 4B). Gel slices corresponding to the position of the bound complexes were excised form the EMSA gels directly for analysis. Samples obtained from the affinity purification were then resolved via SDS-PAGE, and bands present in the lanes incubated with the mismatched substrate, but not in the lanes incubated with the control substrate were cut out and sent for mass-spectrometry identification (Fig. 4C). The excised gel slices from either method were digested under sterile conditions and the peptide profiles analyzed by MALDI-TOF tandem mass spectroscopy. A BLAST-based algorithm (http://www.ncbi.nlm.nih.gov/BLAST) was used to identify candidate proteins in the NCBI non-random database using parameters set to a 99% confidence interval (NIA Mass Spectroscopy unit). Only species detected at least twice were considered. Table 4 lists the results obtained from this analysis.

The top three candidate proteins identified were the pentatricopeptide repeat protein LRP130 (*LRPPRC*), the Y-box binding protein YB-1 (NSEP1, *YBX1*), and a UV-radiation resistance associated protein UVRAG (*UVRRA*). Two known mitochondrial proteins identified with high confidence are also shown (Table 4). LRPPRC was detected both by affinity purification and by non-radioactive EMSA, from a band correlating to a size of approximately 110 kDa, a good match for the actual size of 130 kDa (see material and methods for details). UVRAG and YB-1 were detected in the non-radioactive EMSA but not the affinity purification (Table 4). YB-1 was detected twice in the concentrated lysate derived from the fraction containing species *c*, and once in pooled fraction containing species *a* and *b* (see Fig. S2C for the fractionations). Because YB-1 was detected with high confidence, binds and melts duplex DNA with mismatches or cisplatin DNA crosslinks (Ise *et al.*, 1999;Gaudreault *et al.*, 2004), and has

NIH-PA Author Manuscript

NIH-PA Author Manuscript

NIH-PA Author Manuscript

endo- and exonuclease activity (Gaudreault *et al.*, 2004), YB-1 became the top candidate for investigation as a mitochondrial mismatch binding protein.

Subcellular localization of YB-1

Because mitochondrial localization of YB-1 had not been demonstrated previously, we studied its subcellular distribution using immunocytochemistry. Antibodies against endogenous YB-1 detected most of the protein in the nucleus, but cytoplasmic localization was also clearly detected (Fig 5A). Most of the cytoplasmic signal co-localized significantly with the MitoTracker Red dye (more than 80%, shown as yellow) in cells stressed with excess thymidine, showing that YB-1 does localize to the mitochondrion in HeLa cells. Mitochondrial localization of YB-1 in the absence of thymidine was also observed, although to a lesser degree (Fig. S3). The specificity of the YB-1 antibody in immunofluorescence was tested using siRNA knockdown of YB-1, which decreases the mitochondrial YB-1 signal to undetectable levels compared to the negative control siRNA (not shown).

As a further test, N-terminal GFP-tagged YB-1 (Gaudreault *et al.*, 2004) was ectopically expressed in HeLa cells, and the cells then thymidine-challenged as before. Live fluorescent imaging was taken 24 h after transfection (Fig. 5B). While some cells expressed extremely high levels of YB-1 (bright green cells in the middle of the field), which saturated the signal, mitochondrial localization of the GFP-tagged YB-1 was clearly detected in the cells with lower levels of expression (indicated by arrow). In those cells, the GFP-tagged protein significantly co-localized with the MitoTracker red signal. This represents the first reported localization of YB-1 to mitochondria in human cells.

DNA binding specificity of purified YB-1

To determine whether YB-1 could account for the mismatch binding observed with mitochondrial extracts we investigated the binding specificity of purified GST-YB-1 (Izumi *et al.*, 2001). EMSA binding conditions followed a previously published protocol (Machwe *et al.*, 2002) for recombinant YB-1. Under these conditions, YB-1 bound strongly to the duplex DNA containing a +1 IDL (Fig. 5C, lane 8) but not to the control homoduplex DNA (lane 5). A Y-box containing oligonucleotide (cognate substrate for YB-1 binding) was used as positive control (lane 2). GST control reactions showed no binding to any of the substrates (lanes 3, 6, and 9). Therefore, recombinant YB-1 can bind specifically to a mismatched substrate *in vitro*.

To verify whether YB-1 contributes to DNA mismatch binding in mitochondria *in vivo* we generated YB-1-deficient cells, in which YB-1 levels were decreased via siRNA knockdown. Significant decrease in YB-1 levels was observed with duplexes E3 and with a pool of duplexes 2, 3 and 5 (Fig. 6A) (see Methods). For the binding studies, cells were treated with the pooled duplexes (E235) and mitochondria isolated as previously described. Absence of nuclear contamination of the mitoplast extracts were confirmed by WB, using Lamin B as a nuclear marker (Fig. 6B). To rule out off-target siRNA effects of the knockdown causing differential binding, mitochondrial extracts from HeLa cells not treated with siRNA were also immunodepleted (ID) using either control IgG or anti-YB-1 antibodies (Fig. 6C). These YB-1-deficient mitochondrial extracts were then tested for mismatch binding by EMSA (Fig. 6D). The size-determination described previously (Fig. S2A and B) suggested that species c was most likely to be YB-1. Binding activity of species *c* (the lower band) was clearly reduced in both the YB-1-immunodepletd and the YB-1 KD mitochondrial extracts (compare lanes 2 and 3, immunodepleted, and 4 and 5, knockdown). Moreover, some decrease in the binding activity of species *a* was also observed in the immunodepleted samples. Therefore, by both methods, at least one of the mismatch-specific bands was abrogated by the loss of YB-1, suggesting that YB-1 does bind mismatched DNA in human mitochondria.

NIH-PA Author Manuscript

NIH-PA Author Manuscript

NIH-PA Author Manuscript

YB-1 depletion abrogates HeLa mitochondrial mismatch repair

Thus, we hypothesized that YB-1 participates in MMR in mitochondria, likely in the mismatch binding step. In order to directly demonstrate that YB-1 participates in mitochondrial mismatch repair we performed *in vitro* MMR assays with HeLa mitochondrial extracts depleted of YB-1 by either siRNA knockdown or immunodepletion (as above). Figure 7A presents the results (black bars). For comparison, we also included HeLa WCE, LoVo WCE, positive and negative controls, respectively. HeLa mitochondrial extracts showed 33.1% repair, which was significantly decreased in extracts fromYB-1 KD mitochondria to only 10.8 %repair activity. Similarly, extracts immunodepleted of YB-1 also showed almost 2-fold decrease in repair, to 14.3%, while extracts depleted with pre-immune IgG (HeLa ME Con ID) showed similar levels of repair (32.3%) as the untreated HeLa mitochondrial extracts. These results correlate with the decreased mismatch binding activity of YB-1-depleted mitochondrial extracts (Fig. 6D) and suggest that YB-1 is involved MMR in mitochondria. We thus tested this hypothesis by complementing YB-1-depleted extracts with recombinant GST-YB-1 (HeLa ME YB-1 ID + YB-1). Addition of recombinant YB-1 restored normal levels of MMR, to 35.7%. Addition of GST alone (HeLa ME YB-1 ID + GST) did not complement the lowered repair in the YB-1 depleted extracts; and in fact, it further decreased the MMR activity to 4.6%, possibly due to the GST binding and sequestering other relevant MMR factors. Together, the results presented above clearly demonstrate that YB-1 is involved in mitochondrial MMR in cell lysates.

In order to rule out the contribution of nuclear MMR activity to the repair rates we were detecting, we performed similar repair assays in presence of aphidicolin (Fig. 7A, hatched bars). This antibiotic inhibits the nuclear DNA polymerases α and δ, but not the mitochondrial DNA polymerase γ (Krokan *et al.*, 1979), thus abrogating nuclear MMR, but not mitochondrial MMR. Aphidicolin treatment significantly inhibited repair activity in the HeLa WCE (from 59 to 7.8%), but not the LoVo WCE or any of the mitochondrial extracts. These results dissociate the mitochondrial MMR activity detected from the nuclear MMR repair pathway. Together with our previous observation that the mitochondrial MMR is significantly inhibited by ethidium bromide (Fig 1C), our results indicate that the mitochondrial MMR is a distinct repair pathway, that involves YB-1 and DNA pol γ.

To validate the mitochondrial mismatch repair activity detected using the M13 assay, we tested the same extracts for their ability to promote repair of a dG/T mismatched plasmid substrate (with a 5′ nick) by restriction analysis (Fig. 7B). In this assay, repair of the mismatched substrate regenerates a unique restriction site, which can then be identified by specific restriction digestion (marked with an asterisk) (Wang *et al.*, 2003). DNA mismatch repair activity was calculated by determining the proportion of recovered replicates for each sample that showed the specific digestion pattern expected if the dG/T mismatch was accurately correct. Mismatched DNA incubated with either HeLa WCE or HeLa ME showed repair in five out of eight recovered samples (63%), whilst the LoVo WCE showed no significant repair. YB-1 depletion recapitulated the decrease in repair activity, as YB-1 knockdown HeLa ME gave repair in only three out of eight samples (38%); again indicating that YB-1 directly participates in mediating the repair reaction studied.

Mutations in the mtDNA are expected to affect the respiratory chain and the oxidative phosphorylation system since the mtDNA encodes 13 regulatory subunits of 4 of 5 respiratory complexes. Thus, MMR, by preventing accumulation of mutations in the mtDNA, would promote stability of the respiratory complexes. We reasoned that if MMR is important for maintenance of mitochondrial respiration, its abrogation via YB-1 depletion should impair mitochondrial respiration. We tested this hypothesis by measuring cellular respiration using a fluorescent microplate assay (see Methods) (Fig. 7C). This assay measures the amount of O_2 dissolved in the medium, such that the more O_2 dissolved the lower the normalized relative fluorescence unit (NRFU). In epithelial derived cells, like HeLa, oxygen consumption is almost

NIH-PA Author Manuscript

NIH-PA Author Manuscript

NIH-PA Author Manuscript

exclusively of mitochondrial origin. Thus, NRFU is a direct measure of mitochondrial respiration. Control HeLa cells showed a significant respiration rate (0.28) when compared to the no-cells negative control (0.045). Cells transfected with a non-targeting siRNA (Neg KD) showed a decrease in mitochondrial respiration, likely reflecting the off-target effects of the negative control siRNA and the transfection reagent. On the other hand, YB-1 siRNA transfected cells showed more than two-fold decrease in respiration compared to the control cell (from 0.28 to 0.12), and about 40% (from 0.19 to 0.12) compared to the Neg KD. While indirect, these results indicate that YB-1 KD impair mitochondrial respiration, suggesting accumulation of mtDNA mutations. Since YB-1 is an important transcription factor for general gene expression, these experiments were performed 7 days after siRNA transfection (when YB-1 levels are back to normal, not shown) to avoid changes in respiration indirectly caused by lower cellular metabolism. Thus, changes in respiration are likely due to mutation in the mtDNA that accumulated during the period in which YB-1 levels were abrogated.

YB-1 dependent MMR prevents mtDNA mutagenesis

MMR is thought to contribute to genomic stability by preventing mutations resulting from the replication of mismatched or looped DNA. Thus, if MMR is impaired, mutation rates should increase. We reasoned that if YB-1 was important for mtMMR, mtDNA mutation rate should be higher in its absence. We tested this hypothesis using a chloramphenicol (CAP)-resistance selection assay to select for mtDNA mutants. Chloramphenicol inhibits mitochondrial protein synthesis by binding to ribosomal RNAs (Kroon, 1965). Mutations in the mt-ribosomal RNA genes lead to CAP-resistance in yeast (Bolotin-Fukuhara, 1979) as well as in mammalian cells (Coon and Ho, 1977), and can thus be identified and quantified in selection growth medium containing high concentrations of CAP. Thus, we used a selection in presence of 300 μg/ml CAP, which we determined as a dose that kills more than 95% of HeLa cells (not shown). To validate the assay as measuring mtDNA mutations, we treated HeLa cells with increasing concentrations of Antimycin A (AA), an antibiotic that binds to the ubiquinone reduction site and increases intramitochondrial superoxide anion production (Turrens *et al.*, 1985;Sun and Trumpower, 2003). Figure 8A shows that AA causes a dose-dependent, significant increase in CAP-resistant colonies, up to 3 fold increase in cells treated with 0.6 and 1 μM AA. These results indicate that AA-induced intramitochodrial oxidative stress causes accumulation of mutations in the mtDNA, which reflects in an increase in CAP-resistant colonies, thus validating the assay as a measure of mtDNA mutagenesis.

In order to test the hypothesis that YB-1 plays a direct role in mtMMR and maintenance of mtDNA stability we abrogated intracellular YB-1 levels via siRNA knockdown, as described earlier. Seventy-two hours after the siRNA transfection the cells were replated and selected for CAP-resistance. Figure 8B shows a picture of a representative assay. In this assay, wells 2, 4 and 6 were grown in presence of CAP, while wells 1, 3 and 5 were not to measure plate efficiency. The cultures in which YB-1 levels were decreased (wells 4 and 6) show more CAP-resistant colonies than the mock-transfect cells (well 2), while the plate efficiency was similar to all experimental condition (compare well 1, 3 and 5). These results are quantified in Figure 8C, and show that YB-1 knockdown increases mtDNA mutagenesis by up to 3 fold. Thus, these results indicate that YB-1 prevents mtDNA mutagenesis.

DISCUSSION

This study demonstrates for the first time that human mitochondrial extracts support mismatch repair, in a pathway that is independent of nuclear MMR factors. We also identify a mitochondrial activity that specifically binds base mismatches and small IDLs. This activity is found in both normal human (GM1310) and cancerous (HeLa) cells, indicating that it is not cell type-specific. We identified the transcription/repair factor YB-1 in the mismatched DNA

NIH-PA Author Manuscript

NIH-PA Author Manuscript

NIH-PA Author Manuscript

bound complex, and showed that YB-1 binds mismatched DNA and directly participates in the repair of circular mismatched substrates *in vitro*. More importantly, we show that YB-1 abrogation in cells cause an increase in mtDNA mutagenesis, directly implicating this protein in preventing mutations and maintaining mtDNA stability.

Several lines of evidence presented here support that mitochondrial MMR functions separately from nuclear MMR and does not involve some of the proteins known to function in nuclear MMR. Specifically, our results indicate that MSH2, MSH3, MLH1 and MSH6 are not present in human mitochondria; and MSH2 does not contribute to the mismatch binding activity detected in mitochondrial extracts. The mitochondrial mismatch-binding activity described was distinct from and independent of the essential nuclear repair complexes MutSα and MutSβ, based on the following data: nuclear mismatch repair proteins were not detected by immunofluorescence in HeLa mitochondria (Fig. 2), *Msh2*-deficient cells retain mitochondrial mismatch binding (Fig. 3E), and there is little difference in mitochondrial binding in MSH3 or MSH6 complemented HHUA mitochondrial lysates (Fig. S1). Further, nuclear DNA from *Msh6*-deficient cells shows a higher rate of mutation upon challenge than does wild type, but this is not the case for mtDNA in this comparison (Marcelino *et al.*, 1998).

Mismatch repair catalysed by mitochondrial extracts is inhibited by ethidium bromide but not by aphidicolin. The mitochondrial DNA polymerase γ is highly sensitive to inhibition by ethidium bromide (Tarrago-Litvak *et al.*, 1978), but not by aphidicolin (Krokan *et al.*, 1979). These results implicate pol γ in mtMMR and exclude the contribution of nuclear DNA polymerases to the MMR activity we measured here. Moreover, the mismatch binding patterns obtained with HeLa mitochondrial lysates differed significantly from that of nuclear or whole cell lysate. Thus, the repair activity we describe is unlikely to derive from non-mitochondrial enzymes.

The mitochondrial mismatch binding activity identified here appears to specifically recognize and bind small distortions in the DNA (Fig. 3) rather than a specific sequence context. DNA glycosylase involvement is unlikely since some of the substrates used are not recognized by any known mitochondrial glycosylase. This is the case, for example, for the dG/dG mismatch, which is well-recognized by the activity detected here. Further, an antibody to thymidine DNA glycosylase (which could bind the dG/T mismatches) did not supershift any protein-DNA complexes in the EMSA assays (not shown). We have also excluded that the mismatch-binding activity is due to Topoisomerase I since the bound complex was dissociated by heat, indicating that it is not covalent in nature as the Top-DNA complex is (Yeh *et al.*, 1994) (data not shown). However, we cannot rule out the possibility that proteins that participate in mitochondrial BER may also be involved downstream of the mismatch binding step in the MMR reaction (Larsen *et al.*, 2005).

Our data suggest that the multifunctional YB-1 protein plays a key role in mtMMR. The *in vitro* MMR capacity of mitochondrial extracts correlated well with the presence of YB-1 (Fig. 7A); extracts lacking YB-1 showed less MMR activity, which was complemented upon addition of recombinant YB-1. Although not previously described as mitochondrial, we show clear evidence that a proportion of YB-1 does localize to this organelle in human cells. Immunofluorescence images of both endogenous YB-1 protein (Fig. 5A) as well as GFP-tagged protein (Fig. 5B) clearly co-localize with MitoTracker Red, a marker of mitochondria localization. Moreover, Western blot analysis of highly purified mitoplast lysates detected YB-1 (Fig. 6C), and this band could be specifically depleted from mitochondrial extracts after incubation with an anti-YB-1 antibody. We therefore conclude that YB-1 is present in mitochondria.

NIH-PA Author Manuscript

NIH-PA Author Manuscript

NIH-PA Author Manuscript

YB-1 has been reported to play a direct role in other DNA repair pathways: it stably interacts with and stimulates the catalysis of the BER glycosylase NEIL2, as well as interacting with various other nuclear DNA repair proteins, such as Pol β and APE1 (Das *et al.*, 2007). Also, it binds and melts mismatched DNA substrates, but not homoduplex DNA, and YB-1 can also melt cisplatin cross-linked DNA *in vitro* (Gaudreault *et al.*, 2004). Previous data from our laboratory shows that CHO mitochondria proficiently repair at least some types of interstrand crosslinks (LeDoux *et al.*, 1992) via a pathway yet unidentified. Therefore, it is possible that YB-1 plays a role in the repair of cisplatin adducts in mtDNA as well. While YB-1's stimulation of BER has not been directly linked to any enzymatic activity, but rather to protein-protein interactions, the biochemical activities described above could play important roles in mtMMR. YB-1's ability to bind and discriminate mismatched DNA gives it the ability to work as the mismatch-sensing step in mtMMR. Once bound to the DNA, YB-1 could then function to assemble a "mismatch repairosome" at the mismatch site through specific protein-protein interactions, which could or not involve some of the known BER proteins, to catalyze downstream steps in MMR. It is also of note that YB-1's ability to melt mismatch-containing DNA could function as signal for further steps in the repair process by creating a local distortion in the helix.

Our results show that mitochondrial extracts efficiently bind small IDL's and base mismatches (Fig. 3A). Recombinant purified GST-YB-1, also binds to mismatches (not shown) and +1DL loops (Fig. 5C). In the nuclear MMR pathway, mismatches are recognized and bound by the MutSα and MutSβ heterodimers, which then target the lesions to downstream enzymes for processing. Thus, it is possible that YB-1 exerts a similar function in mitochondria, by recognizing and binding to the mismatched/looped DNA, and targeting these to repair. YB-1 has been shown to physically interact with several DNA repair proteins; it remains to be determined if it interacts with mitochondrial DNA repair proteins, in a fashion that could direct the mismatches/loops for further processing. Because YB-1 has a weak nuclease activity *in vitro* (Gaudreault *et al.*, 2004), it might also perform a mismatch-editing function.

Our results directly implicate YB-1 in maintaining mtDNA stability. We show that YB-1 depletion causes a significant (3-fold) increase in mtDNA mutations, as detected by an increase in the number or CAP-resistant colonies (Fig. 8C). Since YB-1 was identified in the mismatch-bound complex obtained from mitochondrial extracts, and YB-1 depletion also decreases *in vitro* MMR activity of mitochondrial extracts, together these results provide strong evidence for the direct involvement of YB-1 in mitochondrial MMR, likely as the mismatch recognition-binding factor. Moreover, the respiration data presented in Figure 7C shows that YB-1 depletion causes a significant impairment of cellular respiration, which again suggests a role for this protein in mtDNA maintenance. While YB-1 is also a general transcription factor, it is unlike that the decrease in MMR activity we see in extracts depleted of YB-1 are indirect, caused by losing the transcriptional activity of YB-1. We observed a full complementation of the MMR deficiency of extracts immunodepleted of YB-1 when recombinant GST-YB-1 was added back to the extracts (Fig. 7A), thus associating the lower MMR activity with loss of YB-1 itself.

This study also identified LRP130 and UVRAG as possible mismatch-binding proteins in a mitochondrial MMR pathway. LRP130 is a mitochondrial matrix protein involved in splicing cytochrome C oxidase mRNA and may be considered a chaperone (Mootha *et al.*, 2003;Xu *et al.*, 2004;Tsuchiya *et al.*, 2004). Deficiency in LRP130 causes a variant form of a classical mitochondrial disease, Leigh's syndrome, named French-Canadian Leigh's syndrome after the region from where it was identified. Interestingly, LRP130 was identified in a screen of proteins that bind to minisatellite DNA in mouse cells (Tsuchiya *et al.*, 2002), indicating a possible role in genomic stability maintenance. Little is known about UVRAG except that it can partially complement the UV-sensitivity of Xeroderma Pigmentosum complementation group C (Teitz

NIH-PA Author Manuscript

NIH-PA Author Manuscript

NIH-PA Author Manuscript

et al., 1990;Chang *et al*., 2000). One study also shows that the *UVRRG* gene is mutated in colon cancer cells with MSI (Ionov *et al.*, 2004), however mitochondrial localization of the gene product has not yet been demonstrated. Future studies are required to establish mitochondrial localization of this protein, and to determine in what capacity this protein, along with LRP130, participate in mitochondrial MMR.

We show here that human mitochondria have a novel, robust MMR activity, and that this pathway involves YB-1. This significantly extends our understanding about DNA repair functions in mitochondria, where there has been quite limited insight. The multi-functional protein YB-1 localizes to mitochondria and binds mismatched DNA *in vitro*. This study directly implicates YB-1 in mtDNA maintenance, likely via its mismatch binding activity and role in MMR in mitochondria in human cells. These results provide the first direct experimental evidence that mammalian mitochondria are proficient in a novel MMR pathway that may be important in promoting mtDNA stability and in preventing mitochondrial dysfunction and disease.

Supplementary Material

Refer to Web version on PubMed Central for supplementary material.

Acknowledgments

FUNDING

This work (PM, KH, LW, JT, NSP, and VB) was funded by the Intramural Research Program of the National Institutes of Health, National Institute on Aging, USA. TS and LJR are supported by the Danish Cancer Society (grant DP05118). ML was supported partly by a grant from the Cancer Research Society Inc. and is a CIHR scholar, and DG is an NSERC of Canada scholar.

We thank Dr. Stella Martomo for critical reading of the manuscript; Dr. T. Wilson for supplying purified human MutSα protein; Dr. T. J. Kinsella for the human HEC59 and HEC59/2–4 cell lines, Dr T. Kunkel for the HHUA cell lines and Dr. R.N. Lightowlers for the dG/dG3′ M13 substrate. Acknowledgements also to Dr. J. Jiricny for helpful discussion, Dr. F. Indig and Alfred May for microscope training, Dr. S. Saxena for mass spectrometry, Nina Oestergaard Knudsen for the restriction-based MMR assay, and Cynthia Kasmer for cell culture.

ABBREVIATIONS

AA
antimycin A

CAP
chloramphenicol

COXIV
cytochrome oxidase sub-unit IV

EMSA
electromobility shift assay

MALDI-TOF
matrix-assisted laser desorption/ionization–time of flight

ME
mitochondrial extract

MMR
mismatch repair

NIH-PA Author Manuscript

NIH-PA Author Manuscript

NIH-PA Author Manuscript

MP
mitoplast

MSI
microsatellite instability

mtDNA
mitochondrial DNA

mtMMR
mitochondrial mismatch repair

siRNA
small interfering ribonucleic acid

WCE
whole cell extract

YB-1
Y-box binding protein 1

References

1. Acharya S, Wilson T, Gradia S, Kane MF, Guerrette S, Marsischky GT, Kolodner R, Fishel R. hMSH2 forms specific mispair-binding complexes with hMSH3 and hMSH6. Proc Natl Acad Sci U S A 1996;93:13629–13634. [PubMed: 8942985]
2. Alazzouzi H, Farriol M, Espin E, Armengol M, Pena M, Zeh K, Schwartz S, Schwartz S Jr. Molecular patterns of nuclear and mitochondrial microsatellite alterations in breast tumors. Oncol Rep 2003;10:1561–1567. [PubMed: 12883742]
3. Anderson S, Bankier AT, Barrell BG, de Bruijn MH, Coulson AR, Drouin J, Eperon IC, Nierlich DP, Roe BA, Sanger F, Schreier PH, Smith AJ, Staden R, Young IG. Sequence and organization of the human mitochondrial genome. Nature 1981;290:457–465. [PubMed: 7219534]
4. Bannikova S, Zorov DB, Shoeman RL, Tolstonog GV, Traub P. Stability and association with the cytomatrix of mitochondrial DNA in spontaneously immortalized mouse embryo fibroblasts containing or lacking the intermediate filament protein vimentin. DNA Cell Biol 2005;24:710–735. [PubMed: 16274293]
5. Ben Yehuda A, Globerson A, Krichevsky S, Bar OH, Kidron M, Friedlander Y, Friedman G, Ben Yehuda D. Ageing and the mismatch repair system. Mech Ageing Dev 2000;121:173–179. [PubMed: 11164471]
6. Bianchi NO, Bianchi MS, Richard SM. Mitochondrial genome instability in human cancers. Mutat Res 2001;488:9–23. [PubMed: 11223402]
7. Bohr VA. Repair of oxidative DNA damage in nuclear and mitochondrial DNA, and some changes with aging in mammalian cells. Free Radic Biol Med 2002;32:804–812. [PubMed: 11978482]
8. Bolotin-Fukuhara M. Mitochondrial and nuclear mutations that affect the biogenesis of the mitochondrial ribosomes of yeast. I. Genetics. Mol Gen Genet 1979;177:39–46. [PubMed: 395414]
9. Boyer JC, Umar A, Risinger JI, Lipford JR, Kane M, Yin S, Barrett JC, Kolodner RD, Kunkel TA. Microsatellite instability, mismatch repair deficiency, and genetic defects in human cancer cell lines. Cancer Res 1995;55:6063–6070. [PubMed: 8521394]
10. Buermeyer AB, Deschenes SM, Baker SM, Liskay RM. Mammalian DNA mismatch repair. Annu Rev Genet 1999;33:533–564. [PubMed: 10690417]
11. Chang DK, Ricciardiello L, Goel A, Chang CL, Boland CR. Steady-state regulation of the human DNA mismatch repair system. J Biol Chem 2000;275:18424–18431. [PubMed: 10747992]
12. Chi NW, Kolodner RD. Purification and characterization of MSH1, a yeast mitochondrial protein that binds to DNA mismatches. J Biol Chem 1994a;269:29984–29992. [PubMed: 7961998]

NIH-PA Author Manuscript NIH-PA Author Manuscript NIH-PA Author Manuscript

13. Chi NW, Kolodner RD. The effect of DNA mismatches on the ATPase activity of MSH1, a protein in yeast mitochondria that recognizes DNA mismatches. J Biol Chem 1994b;269:29993–29997. [PubMed: 7961999]
14. Claij N, te RH. Msh2 deficiency does not contribute to cisplatin resistance in mouse embryonic stem cells. Oncogene 2004;23:260–266. [PubMed: 14712231]
15. Clayton DA, Doda JN, Friedberg EC. The absence of a pyrimidine dimer repair mechanism in mammalian mitochondria. Proc Natl Acad Sci U S A 1974;71:2777–2781. [PubMed: 4212385]
16. Coon HG, Ho C. Transformation of cultured cells to chloramphenicol resistance by purified mammalian mitochondrial DNA. Brookhaven Symp Biol 1977:166–177. [PubMed: 754863]
17. Copeland WC, Longley MJ. DNA polymerase gamma in mitochondrial DNA replication and repair. ScientificWorldJournal 2003;3:34–44. [PubMed: 12806118]
18. Croteau DL, ap Rhys CM, Hudson EK, Dianov GL, Hansford RG, Bohr VA. An oxidative damage-specific endonuclease from rat liver mitochondria. J Biol Chem 1997;272:27338–27344. [PubMed: 9341184]
19. Das S, Chattopadhyay R, Bhakat KK, Boldogh I, Kohno K, Prasad R, Wilson SH, Hazra TK. Stimulation of NEIL2-mediated oxidized base excision repair via YB-1 interaction during oxidative stress. J Biol Chem 2007;282:28474–28484. [PubMed: 17686777]
20. Dianov GL, Souza-Pinto N, Nyaga SG, Thybo T, Stevnsner T, Bohr VA. Base excision repair in nuclear and mitochondrial DNA. Prog Nucleic Acid Res Mol Biol 2001;68:285–297. [PubMed: 11554304]
21. Dignam JD, Lebovitz RM, Roeder RG. Accurate transcription initiation by RNA polymerase II in a soluble extract from isolated mammalian nuclei. Nucleic Acids Res 1983;11:1475–1489. [PubMed: 6828386]
22. Fang DC, Fang L, Wang RQ, Yang SM. Nuclear and mitochondrial DNA microsatellite instability in hepatocellular carcinoma in Chinese. World J Gastroenterol 2004;10:371–375. [PubMed: 14760760]
23. Fang WH, Modrich P. Human strand-specific mismatch repair occurs by a bidirectional mechanism similar to that of the bacterial reaction. J Biol Chem 1993;268:11838–11844. [PubMed: 8505312]
24. Fink D, Nebel S, Aebi S, Zheng H, Cenni B, Nehme A, Christen RD, Howell SB. The role of DNA mismatch repair in platinum drug resistance. Cancer Res 1996;56:4881–4886. [PubMed: 8895738]
25. Fliss MS, Usadel H, Caballero OL, Wu L, Buta MR, Eleff SM, Jen J, Sidransky D. Facile detection of mitochondrial DNA mutations in tumors and bodily fluids. Science 2000;287:2017–2019. [PubMed: 10720328]
26. Gaudreault I, Guay D, Lebel M. YB-1 promotes strand separation in vitro of duplex DNA containing either mispaired bases or cisplatin modifications, exhibits endonucleolytic activities and binds several DNA repair proteins. Nucleic Acids Res 2004;32:316–327. [PubMed: 14718551]
27. Genschel J, Littman SJ, Drummond JT, Modrich P. Isolation of MutSbeta from human cells and comparison of the mismatch repair specificities of MutSbeta and MutSalpha. J Biol Chem 1998;273:19895–19901. [PubMed: 9677427]
28. Habano W, Nakamura S, Sugai T. Microsatellite instability in the mitochondrial DNA of colorectal carcinomas: evidence for mismatch repair systems in mitochondrial genome. Oncogene 1998;17:1931–1937. [PubMed: 9788436]
29. Habano W, Sugai T, Nakamura SI, Uesugi N, Yoshida T, Sasou S. Microsatellite instability and mutation of mitochondrial and nuclear DNA in gastric carcinoma. Gastroenterology 2000a;118:835–841. [PubMed: 10784582]
30. Habano W, Sugai T, Nakamura SI, Uesugi N, Yoshida T, Sasou S. Microsatellite instability and mutation of mitochondrial and nuclear DNA in gastric carcinoma. Gastroenterology 2000b;118:835–841. [PubMed: 10784582]
31. Habano W, Sugai T, Yoshida T, Nakamura S. Mitochondrial gene mutation, but not large-scale deletion, is a feature of colorectal carcinomas with mitochondrial microsatellite instability. Int J Cancer 1999;83:625–629. [PubMed: 10521798]
32. Harfe BD, Jinks-Robertson S. DNA mismatch repair and genetic instability. Annu Rev Genet 2000;34:359–399. [PubMed: 11092832]

NIH-PA Author Manuscript NIH-PA Author Manuscript NIH-PA Author Manuscript

33. Indig FE, az-Gonzalez F, Ginsberg MH. Analysis of the tetraspanin CD9-integrin alphaIIbbeta3 (GPIIb-IIIa) complex in platelet membranes and transfected cells. Biochem J 1997;327:291–298. [PubMed: 9355765]
34. Ionov Y, Nowak N, Perucho M, Markowitz S, Cowell JK. Manipulation of nonsense mediated decay identifies gene mutations in colon cancer Cells with microsatellite instability. Oncogene 2004;23:639–645. [PubMed: 14737099]
35. Ise T, Nagatani G, Imamura T, Kato K, Takano H, Nomoto M, Izumi H, Ohmori H, Okamoto T, Ohga T, Uchiumi T, Kuwano M, Kohno K. Transcription factor Y-box binding protein 1 binds preferentially to cisplatin-modified DNA and interacts with proliferating cell nuclear antigen. Cancer Res 1999;59:342–346. [PubMed: 9927044]
36. Izumi H, Imamura T, Nagatani G, Ise T, Murakami T, Uramoto H, Torigoe T, Ishiguchi H, Yoshida Y, Nomoto M, Okamoto T, Uchiumi T, Kuwano M, Funa K, Kohno K. Y box-binding protein-1 binds preferentially to single-stranded nucleic acids and exhibits 3′-->5′ exonuclease activity. Nucleic Acids Res 2001;29:1200–1207. [PubMed: 11222770]
37. Kajander OA, Karhunen PJ, Holt IJ, Jacobs HT. Prominent mitochondrial DNA recombination intermediates in human heart muscle. EMBO Rep 2001;2:1007–1012. [PubMed: 11713192]
38. Kang D, Hamasaki N. Maintenance of mitochondrial DNA integrity: repair and degradation. Curr Genet 2002;41:311–322. [PubMed: 12185497]
39. Kohno K, Izumi H, Uchiumi T, Ashizuka M, Kuwano M. The pleiotropic functions of the Y-box-binding protein, YB-1. Bioessays 2003;25:691–698. [PubMed: 12815724]
40. Kose K, Hiyama T, Tanaka S, Yoshihara M, Yasui W, Chayama K. Somatic mutations of mitochondrial DNA in digestive tract cancers. J Gastroenterol Hepatol 2005;20:1679–1684. [PubMed: 16246185]
41. Kose K, Hiyama T, Tanaka S, Yoshihara M, Yasui W, Chayama K. Nuclear and mitochondrial DNA microsatellite instability in gastrointestinal stromal tumors. Pathobiology 2006;73:93–97. [PubMed: 16943689]
42. Krokan H, Schaffer P, DePamphilis ML. Involvement of eucaryotic deoxyribonucleic acid polymerases alpha and gamma in the replication of cellular and viral deoxyribonucleic acid. Biochemistry 1979;18:4431–4443. [PubMed: 226127]
43. Kroon AM. Protein synthesis in mitochondria. 3. On the effects of inhibitors on the incorporation of amino acids into protein by intact mitochondria and digitonin fractions. Biochim Biophys Acta 1965;108:275–284. [PubMed: 5865510]
44. Kumimoto H, Yamane Y, Nishimoto Y, Fukami H, Shinoda M, Hatooka S, Ishizaki K. Frequent somatic mutations of mitochondrial DNA in esophageal squamous cell carcinoma. Int J Cancer 2004;108:228–231. [PubMed: 14639607]
45. Lakshmipathy U, Campbell C. Double strand break rejoining by mammalian mitochondrial extracts. Nucleic Acids Res 1999;27:1198–1204. [PubMed: 9927756]
46. Larsen NB, Rasmussen M, Rasmussen LJ. Nuclear and mitochondrial DNA repair: similar pathways? Mitochondrion 2005;5:89–108. [PubMed: 16050976]
47. Larsson NG, Clayton DA. Molecular genetic aspects of human mitochondrial disorders. Annu Rev Genet 1995;29:151–178. [PubMed: 8825472]
48. LeDoux SP, Wilson GL, Beecham EJ, Stevnsner T, Wassermann K, Bohr VA. Repair of mitochondrial DNA after various types of DNA damage in Chinese hamster ovary cells. Carcinogenesis 1992;13:1967–1973. [PubMed: 1423864]
49. Lievre A, Chapusot C, Bouvier AM, Zinzindohoue F, Piard F, Roignot P, Arnould L, Beaune P, Faivre J, Laurent-Puig P. Clinical value of mitochondrial mutations in colorectal cancer. J Clin Oncol 2005;23:3517–3525. [PubMed: 15908662]%20
50. Liu B, Nicolaides NC, Markowitz S, Willson JK, Parsons RE, Jen J, Papadopolous N, Peltomaki P, de la CA, Hamilton SR. Mismatch repair gene defects in sporadic colorectal cancers with microsatellite instability. Nat Genet 1995;9:48–55. [PubMed: 7704024]
51. Machwe A, Xiao L, Theodore S, Orren DK. DNase I footprinting and enhanced exonuclease function of the bipartite Werner syndrome protein (WRN) bound to partially melted duplex DNA. J Biol Chem 2002;277:4492–4504. [PubMed: 11717307]

NIH-PA Author Manuscript NIH-PA Author Manuscript NIH-PA Author Manuscript

52. Mandavilli BS, Santos JH, Van Houten B. Mitochondrial DNA repair and aging. Mutat Res 2002;509:127–151. [PubMed: 12427535]
53. Marcelino LA, Andre PC, Khrapko K, Coller HA, Griffith J, Thilly WG. Chemically induced mutations in mitochondrial DNA of human cells: mutational spectrum of N-methyl-N′-nitro-N-nitrosoguanidine. Cancer Res 1998;58:2857–2862. [PubMed: 9661902]
54. Marra G, Schar P. Recognition of DNA alterations by the mismatch repair system. Biochem J 1999;338 (Pt 1):1–13. [PubMed: 9931291]
55. Mason PA, Matheson EC, Hall AG, Lightowlers RN. Mismatch repair activity in mammalian mitochondria. Nucleic Acids Res 2003;31:1052–1058. [PubMed: 12560503]
56. Mootha VK, Lepage P, Miller K, Bunkenborg J, Reich M, Hjerrild M, Delmonte T, Villeneuve A, Sladek R, Xu F, Mitchell GA, Morin C, Mann M, Hudson TJ, Robinson B, Rioux JD, Lander ES. Identification of a gene causing human cytochrome c oxidase deficiency by integrative genomics. Proc Natl Acad Sci U S A 2003;100:605–610. [PubMed: 12529507]
57. Morisawa T. The results of primary culture of endometrial adenocarcinoma and characterization of its established line. J Jpn Soc Clin Cytol 1987;26:433–442.
58. Nagley P, Wei YH. Ageing and mammalian mitochondrial genetics. Trends Genet 1998;14:513–517. [PubMed: 9865158]
59. Parsons R, Li GM, Longley MJ, Fang WH, Papadopoulos N, Jen J, de la CA, Kinzler KW, Vogelstein B, Modrich P. Hypermutability and mismatch repair deficiency in RER+ tumor cells. Cell 1993;75:1227–1236. [PubMed: 8261516]
60. Polyak K, Li Y, Zhu H, Lengauer C, Willson JK, Markowitz SD, Trush MA, Kinzler KW, Vogelstein B. Somatic mutations of the mitochondrial genome in human colorectal tumours. Nat Genet 1998;20:291–293. [PubMed: 9806551]
61. Pont-Kingdon G, Okada NA, Macfarlane JL, Beagley CT, Watkins-Sims CD, Cavalier-Smith T, Clark-Walker GD, Wolstenholme DR. Mitochondrial DNA of the coral Sarcophyton glaucum contains a gene for a homologue of bacterial MutS: a possible case of gene transfer from the nucleus to the mitochondrion. J Mol Evol 1998;46:419–431. [PubMed: 9541536]
62. Reenan RA, Kolodner RD. Characterization of insertion mutations in the Saccharomyces cerevisiae MSH1 and MSH2 genes: evidence for separate mitochondrial and nuclear functions. Genetics 1992;132:975–985. [PubMed: 1334021]
63. Richter C, Park JW, Ames BN. Normal oxidative damage to mitochondrial and nuclear DNA is extensive. Proc Natl Acad Sci U S A 1988;85:6465–6467. [PubMed: 3413108]
64. Sansom OJ, Toft NJ, Winton DJ, Clarke AR. Msh-2 suppresses in vivo mutation in a gene dose and lesion dependent manner. Oncogene 2001;20:3580–3584. [PubMed: 11429706]
65. Schnaitman C, Greenawalt JW. Enzymatic properties of the inner and outer membranes of rat liver mitochondria. J Cell Biol 1968;38:158–175. [PubMed: 5691970]
66. Song S, Wheeler LJ, Mathews CK. Deoxyribonucleotide pool imbalance stimulates deletions in HeLa cell mitochondrial DNA. J Biol Chem 2003;278:43893–43896. [PubMed: 13679382]
67. Sun J, Trumpower BL. Superoxide anion generation by the cytochrome bc1 complex. Arch Biochem Biophys 2003;419:198–206. [PubMed: 14592463]
68. Tan DJ, Bai RK, Wong LJ. Comprehensive scanning of somatic mitochondrial DNA mutations in breast cancer. Cancer Res 2002b;62:972–976. [PubMed: 11861366]
69. Tan DJ, Bai RK, Wong LJ. Comprehensive scanning of somatic mitochondrial DNA mutations in breast cancer. Cancer Res 2002a;62:972–976. [PubMed: 11861366]
70. Tarrago-Litvak L, Viratelle O, Darriet D, Dalibart R, Graves PV, Litvak S. The inhibition of mitochondrial DNA polymerase gamma from animal cells by intercalating drugs. Nucleic Acids Res 1978;5:2197–2210. [PubMed: 673850]
71. Teitz T, Penner M, Eli D, Stark M, Bakhanashvili M, Naiman T, Canaani D. Isolation by polymerase chain reaction of a cDNA whose product partially complements the ultraviolet sensitivity of xeroderma pigmentosum group C cells. Gene 1990;87:295–298. [PubMed: 2332174]
72. Thomas DC, Roberts JD, Kunkel TA. Heteroduplex repair in extracts of human HeLa cells. J Biol Chem 1991;266:3744–3751. [PubMed: 1995629]
73. Thyagarajan B, Padua RA, Campbell C. Mammalian mitochondria possess homologous DNA recombination activity. J Biol Chem 1996;271:27536–27543. [PubMed: 8910339]

NIH-PA Author Manuscript

NIH-PA Author Manuscript

NIH-PA Author Manuscript

74. Tsuchiya N, Fukuda H, Nakashima K, Nagao M, Sugimura T, Nakagama H. LRP130, a single-stranded DNA/RNA-binding protein, localizes at the outer nuclear and endoplasmic reticulum membrane, and interacts with mRNA in vivo. Biochem Biophys Res Commun 2004;317:736–743. [PubMed: 15081402]
75. Tsuchiya N, Fukuda H, Sugimura T, Nagao M, Nakagama H. LRP130, a protein containing nine pentatricopeptide repeat motifs, interacts with a single-stranded cytosine-rich sequence of mouse hypervariable minisatellite Pc-1. Eur J Biochem 2002;269:2927–2933. [PubMed: 12071956]
76. Turrens JF, Alexandre A, Lehninger AL. Ubisemiquinone is the electron donor for superoxide formation by complex III of heart mitochondria. Arch Biochem Biophys 1985;237:408–414. [PubMed: 2983613]
77. Umar A, Boyer JC, Kunkel TA. DNA loop repair by human cell extracts. Science 1994a;266:814–816. [PubMed: 7973637]
78. Umar A, Boyer JC, Thomas DC, Nguyen DC, Risinger JI, Boyd J, Ionov Y, Perucho M, Kunkel TA. Defective mismatch repair in extracts of colorectal and endometrial cancer cell lines exhibiting microsatellite instability. J Biol Chem 1994b;269:14367–14370. [PubMed: 8182040]
79. Umar A, Koi M, Risinger JI, Glaab WE, Tindall KR, Kolodner RD, Boland CR, Barrett JC, Kunkel TA. Correction of hypermutability, N-methyl-N′-nitro-N-nitrosoguanidine resistance, and defective DNA mismatch repair by introducing chromosome 2 into human tumor cells with mutations in MSH2 and MSH6. Cancer Res 1997;57:3949–3955. [PubMed: 9307278]
80. Vaisman A, Varchenko M, Umar A, Kunkel TA, Risinger JI, Barrett JC, Hamilton TC, Chaney SG. The role of hMLH1, hMSH3, and hMSH6 defects in cisplatin and oxaliplatin resistance: correlation with replicative bypass of platinum-DNA adducts. Cancer Res 1998;58:3579–3585. [PubMed: 9721864]
81. Wang H, Hays JB. Mismatch repair in human nuclear extracts: effects of internal DNA-hairpin structures between mismatches and excision-initiation nicks on mismatch correction and mismatch-provoked excision. J Biol Chem 2003;278:28686–28693. [PubMed: 12756259]
82. Wang JC. Cellular roles of DNA topoisomerases: a molecular perspective. Nat Rev Mol Cell Biol 2002;3:430–440. [PubMed: 12042765]
83. Xu F, Morin C, Mitchell G, Ackerley C, Robinson BH. The role of the LRPPRC (leucine-rich pentatricopeptide repeat cassette) gene in cytochrome oxidase assembly: mutation causes lowered levels of COX (cytochrome c oxidase) I and COX III mRNA. Biochem J 2004;382:331–336. [PubMed: 15139850]
84. Yakes FM, Van HB. Mitochondrial DNA damage is more extensive and persists longer than nuclear DNA damage in human cells following oxidative stress. Proc Natl Acad Sci U S A 1997;94:514–519. [PubMed: 9012815]
85. Yeh YC, Liu HF, Ellis CA, Lu AL. Mammalian topoisomerase I has base mismatch nicking activity. J Biol Chem 1994;269:15498–15504. [PubMed: 8195193]

NIH-PA Author Manuscript

NIH-PA Author Manuscript

NIH-PA Author Manuscript

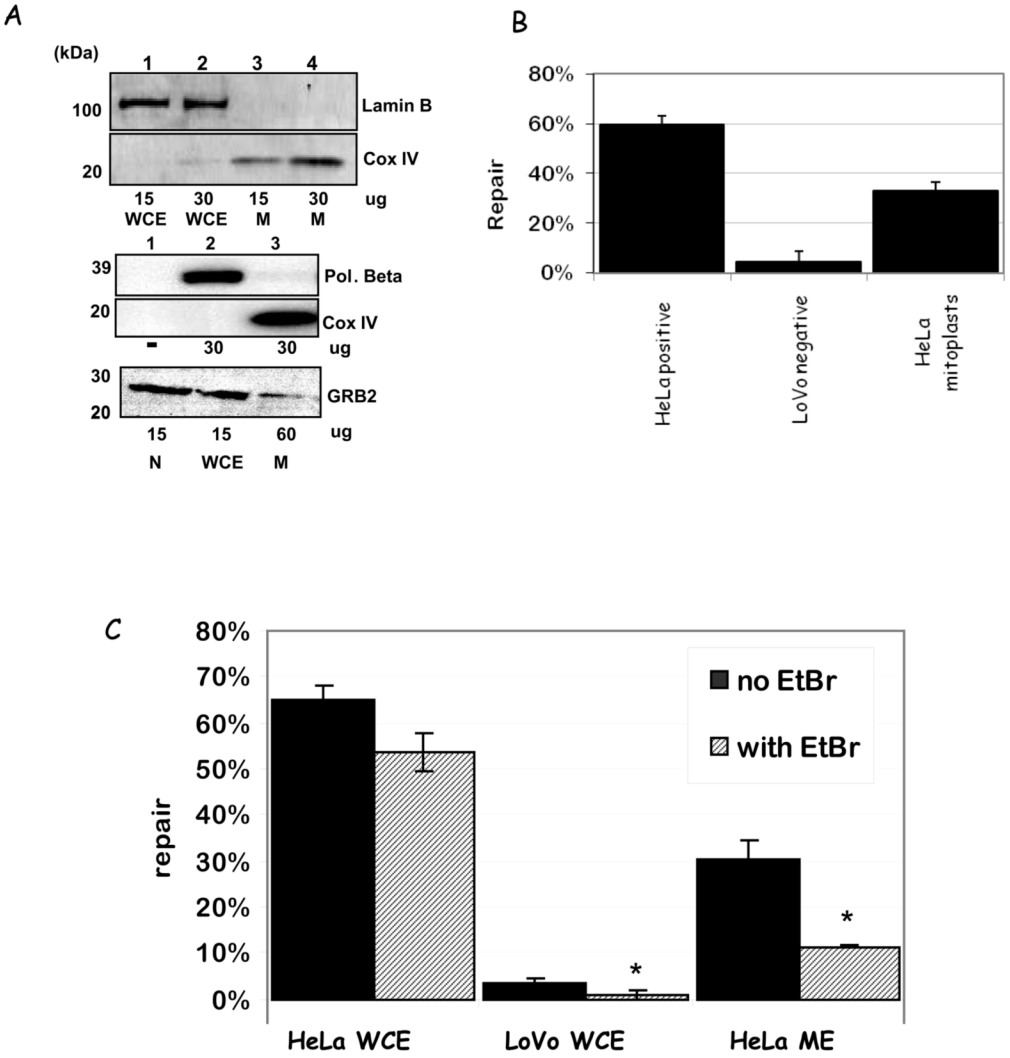

Figure 1.

A. Western blot analysis of mitochondrial purity using Pol β, Lamin B, and GRB2 (nuclear and cytosolic markers, respectively) and COXIV (mitochondrial marker) antibodies. Amounts of protein loaded in the gels are listed bellow the blots; relative % purities (using ImageQuant quantification) are given in the text. **B.** MMR activity using M13 dG/dG mismatched substrate with a 3′ nick with HeLa WCE (HeLa positive), LoVo WCE (LoVo negative) and HeLa ME (HeLa mitoplasts). Results are shown as relative % repair compared to control (mock). N = 3; results are shown as ±SEM. **C.** MMR activity using M13 dG/dG mismatched substrate as before in the absence (black bars) or presence (striped bars) of ethidium bromide, with the same extracts as above. The results presented are average ± SEM of two independent experiments; relevant *p*-values (Student's *t*-test analysis) are given in the text.

NIH-PA Author Manuscript

NIH-PA Author Manuscript

NIH-PA Author Manuscript

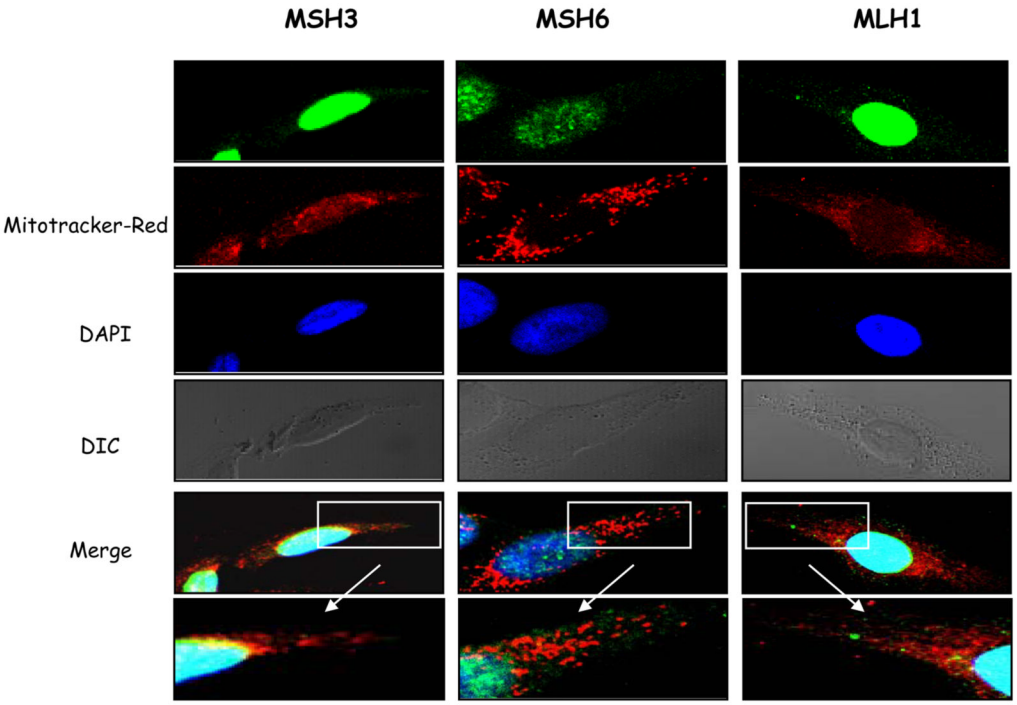

Figure 2.

A. Cellular localization of MMR proteins, MSH3, MSH6 and MLH1 in thymidine-treated HeLa cells. Antibodies against each protein were visualized with AlexaFluor 488-conjugated secondary antibodies (green); mitochondria were labelled with Mitotracker Red (red) and the nuclei with DAPI (blue). DIC and merged images including cytoplasmic details (6–8x zoom) are also shown. Pearson's correlation coefficients are ≤ 0.15 for all samples.

NIH-PA Author Manuscript

NIH-PA Author Manuscript

NIH-PA Author Manuscript

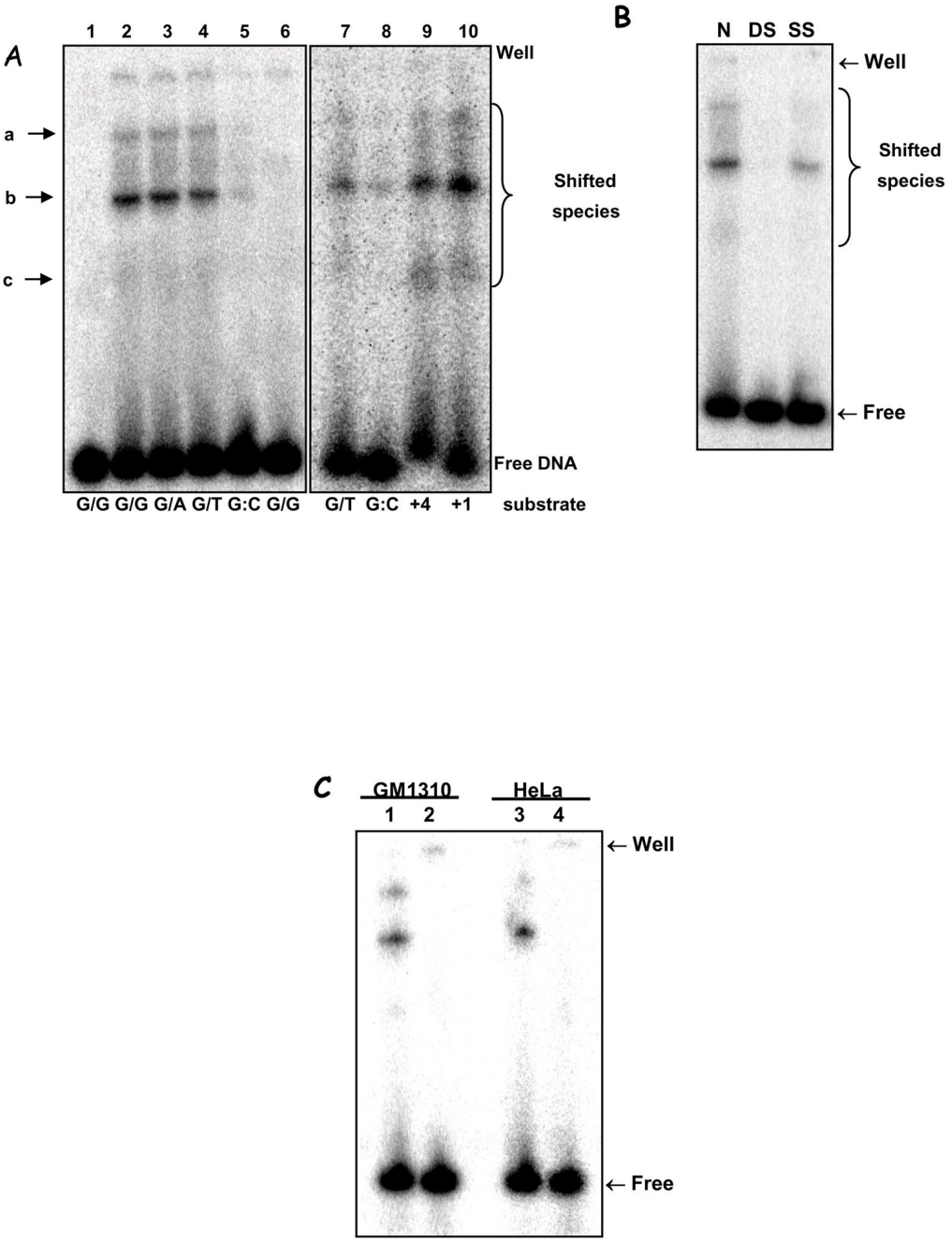

NIH-PA Author Manuscript

NIH-PA Author Manuscript

NIH-PA Author Manuscript

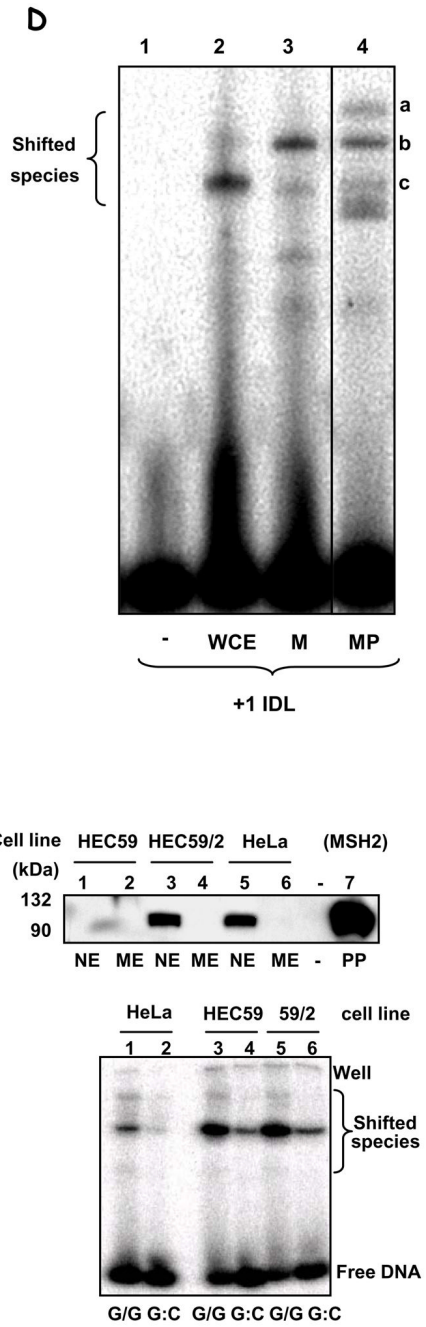

Figure 3.

A. EMSA of mismatch-containing substrate with HeLa mitochondrial extracts. Substrates: dG/dG (L1, 2 & 6), dG/dA (L3), dG/T (L4 & 7), dG:dC (L5 & 8), 4 bp- and 1 bp-insertion (+4 & +1, L9 & 10). L1 shows substrate alone; L6, heat-inactivated lysate ('▲', 95°C, 5 min). Electrophoretic origin: 'well', shifted species, and free substrate are indicated. Binding data is given in the text; N=3, values are mean ±SEM. **B.** Competition assays using unspecific competitor DNA were carried out essentially as in (A), with labelled dG/dG substrate, without (N) or with the addition of 20 ng of each poly[dI-dC]•[dI-dC] (DS), poly[dI-dC] (SS). **C.** EMSA was performed using dG/dG substrate, as in (A), heated at 95°C for 10 min (lanes 2 and 4) or not (lanes 1 and 3), and analyzed as above. Mitochondrial extracts from GM1310 (lanes 1 and

NIH-PA Author Manuscript

NIH-PA Author Manuscript

NIH-PA Author Manuscript

2) or HeLa cells (lanes 3 and 4) were analyzed. **D.** EMSA on +1IDL substrate with HeLa whole cell extract (WCE, lane 2), mitochondrial extract (M, lane 3), or mitoplast extracts (MP, lane 4). Lane 1 is substrate alone. **E.** Top panel: Western blot with hMSH2 antibody of nuclear (NE) and mitochondrial extracts (ME) from HeLa, HEC59 (*msh2*-deficient) and HEC59/2–5 (HEC59 complemented with chromosomes 2 and 4); purified hMutSα protein (L7, as MSH2/MSH6) is included as a positive control for MHS2 as indicated. Sizes are marked. Bottom panel: EMSA with mitochondrial extracts from HeLa (lanes 1 & 2), HEC59 (lanes 3 & 4) and HEC59/2–4 (lanes 5 & 6) cells on dG/dG (lanes 1, 3 & 5) mismatched or control dG:dC (lanes 2, 4 & 6) substrates.

NIH-PA Author Manuscript

NIH-PA Author Manuscript

NIH-PA Author Manuscript

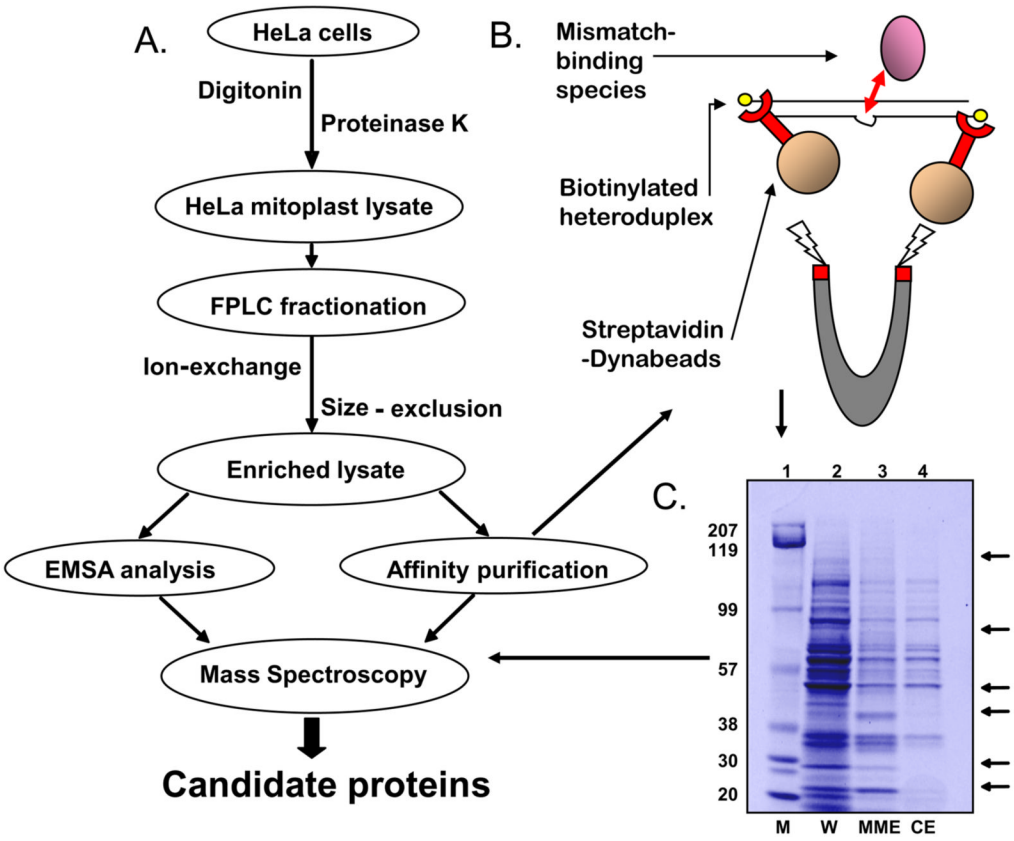

Figure 4.

A. Purification scheme used to identify putative mitochondrial mismatch-binding proteins. B. Depiction of the affinity purification scheme using biotinylated-mismatch substrate and streptavidin-conjugated magnetic beads. C. Representative SDS-PAGE after affinity purification of concentrated lysate after fractionation on biotinylated +1 IDL substrate. Lane 2 = input (W), L3 = mismatch-bound (MME) and lane 4 = homoduplex-bound species (CE). Mismatch-specific species (lane 3) were taken for MS analysis (see arrows). Lane 1 shows the molecular weight markers (M)

NIH-PA Author Manuscript

NIH-PA Author Manuscript

NIH-PA Author Manuscript

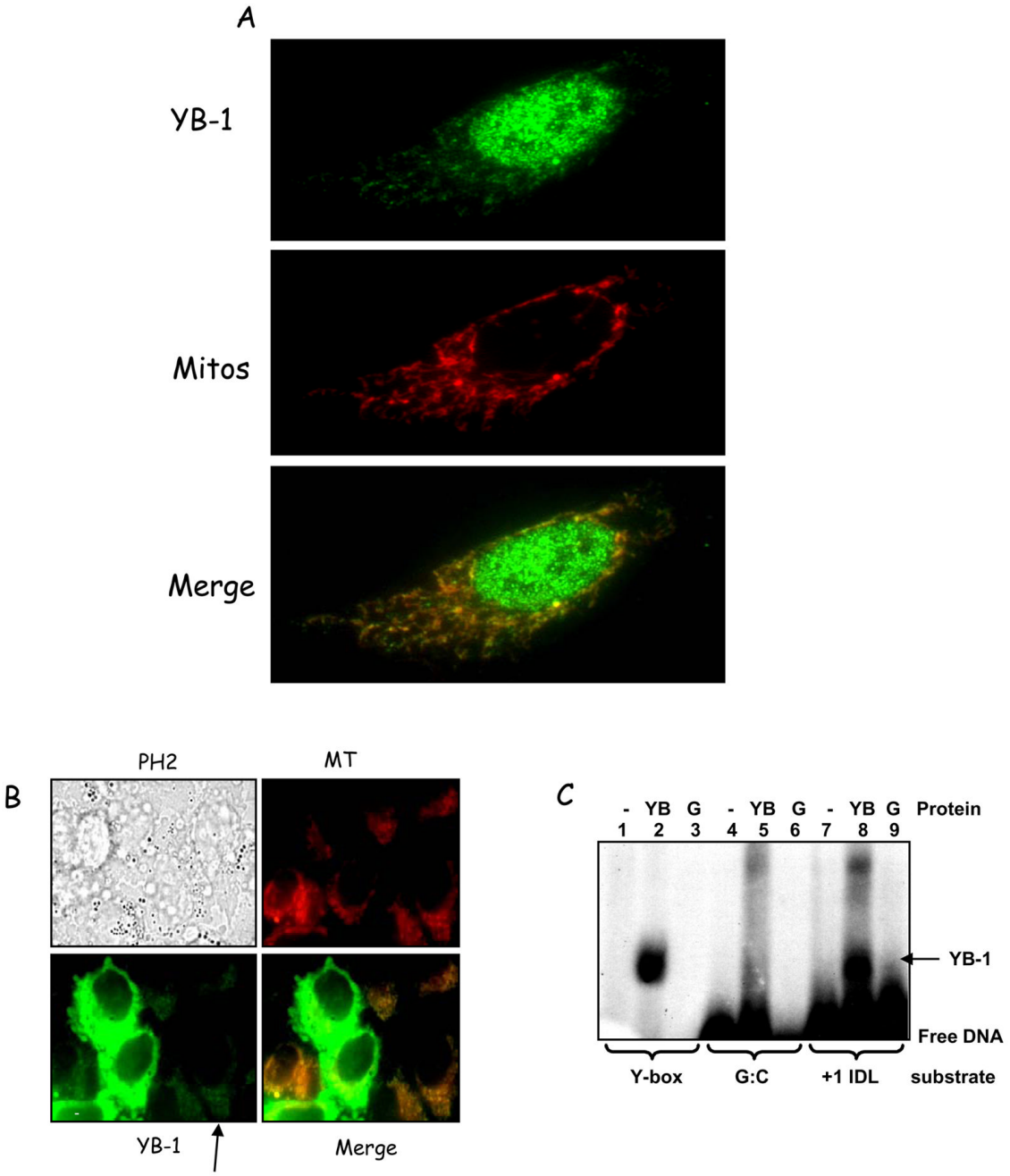

Figure 5.

A. Cellular localization of YB-1 thymidine-stressed HeLa cells. Anti-YB-1 antibody was visualized with AlexaFluor 488 secondary antibody (green). Mitochondria were labelled with MitoTracker Red (red). The merged image shows co-localization appearing as yellow. Pearson's coefficient = 0.626 with stringent threshold. **B.** Thymidine- treated HeLa cells were transfected with GFP-YB-1 (Gaudreault *et al.*, 2004) and incubated with MitoTracker Red for visualizing mitochondria. PH2 = phase contrast (transmitted light) image; MT = MitoTracker red, and YB-1 = transfected GFP-YB-1 signal. Co-localization appears yellow (see 'Merge'). **C.** EMSA with recombinant purified GST-YB-1 (YB) (lanes 2, 5 and 8) or GST alone (G)

(lanes 3, 6 and 9) on +1 IDL (7–9) and G:C (control) (4–6) substrates. A Y-box-containing substrate was also used as positive control (lanes 1–3) (Machwe *et al.*, 2002).

NIH-PA Author Manuscript

NIH-PA Author Manuscript

NIH-PA Author Manuscript

NIH-PA Author Manuscript

NIH-PA Author Manuscript

NIH-PA Author Manuscript

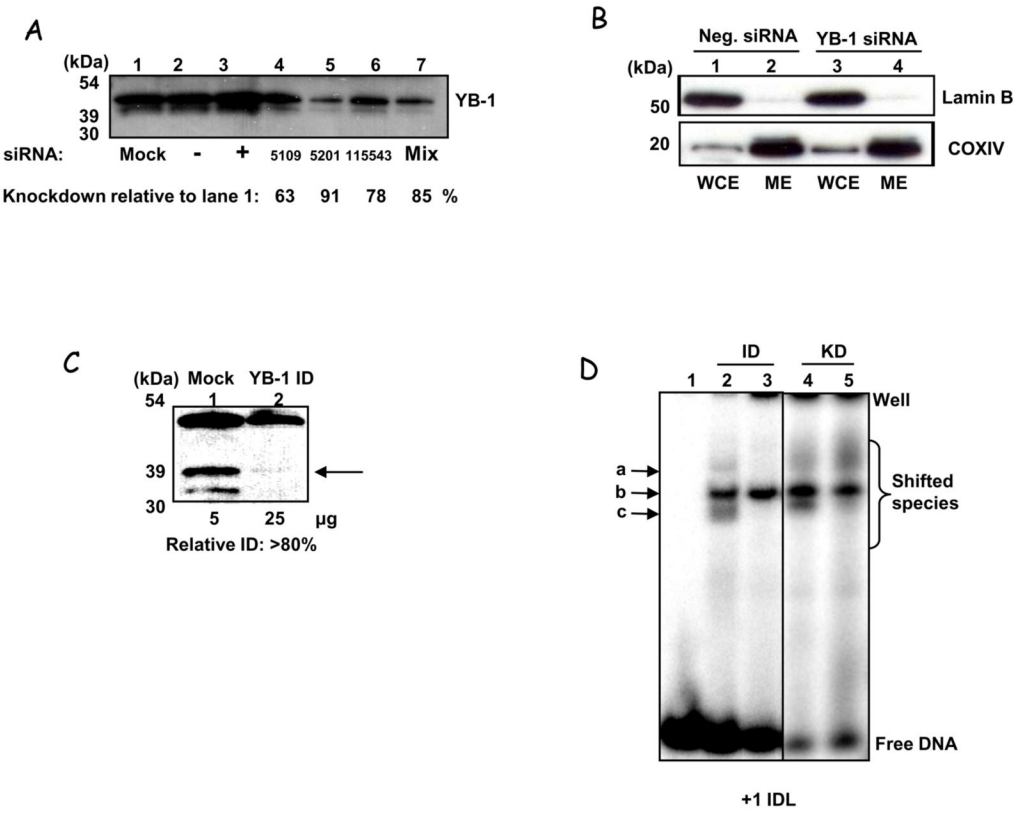

Figure 6.

A. Western analysis of HeLa WCE harvested 72 hrs after YB-1 siRNA knockdown. Even loading was ascertained by staining with DB-71. Lane 1 = mock-transfected, lane 2 = scrambled siRNA; lane 3 = positive control siRNA (Lamin A/C (KD = 70%, data not shown); lanes 4, 5, and 6 have siRNA targeted to exons 2, 3 & 5 of YB-1 respectively, and lane 7 shows knockdown using all three. Levels of YB-1 relative to control cells (lane 1) are given. **B.** Mitoplasts obtained from cells depleted of YB-1 (using the E235 siRNA pool) were tested for purity using Western blot as described in Fig. 1A. Whole cell extracts (WCE) and mitoplast extracts (ME) are shown for both negative control (lanes 1 & 2) and YB-1-siRNA treated (lanes 3 & 4) cells. Size markers are shown (kDa). **C.** Western analysis of HeLa mitochondrial extracts after immunodepletion with anti-YB-1 antibody (lane 2, 'YB-1 ID') or IgG-control (lane 1 'mock'). Amounts of protein loaded in the gel are shown below the blot. **D.** EMSA with mitochondrial extracts mock or YB-1 immunodepleted (lanes 2 & 3, respectively), or extracts from mitochondria obtained from cells transfected with negative or YB-1 siRNA (as above) (lanes 4 & 5, respectively) on the +1 IDL substrate. Quantification for the lower binding species shows around 80% reduction (binding values: ID-control = 4% ± 0.42, YB-1-ID = 0.72% ± 1.3; KD control is 7.2% = 0.21, YB-1-KD = 1.6% ± 0.83 (SEM), N=3 for ID & N=2 for KD). The differences between each +/− YB-1 lysate were analysed by Student's *t*-test and were significant for both: ID, $p = 2.93\times10^{-4}$, KD, $p = 0.022$.

NIH-PA Author Manuscript

NIH-PA Author Manuscript

NIH-PA Author Manuscript

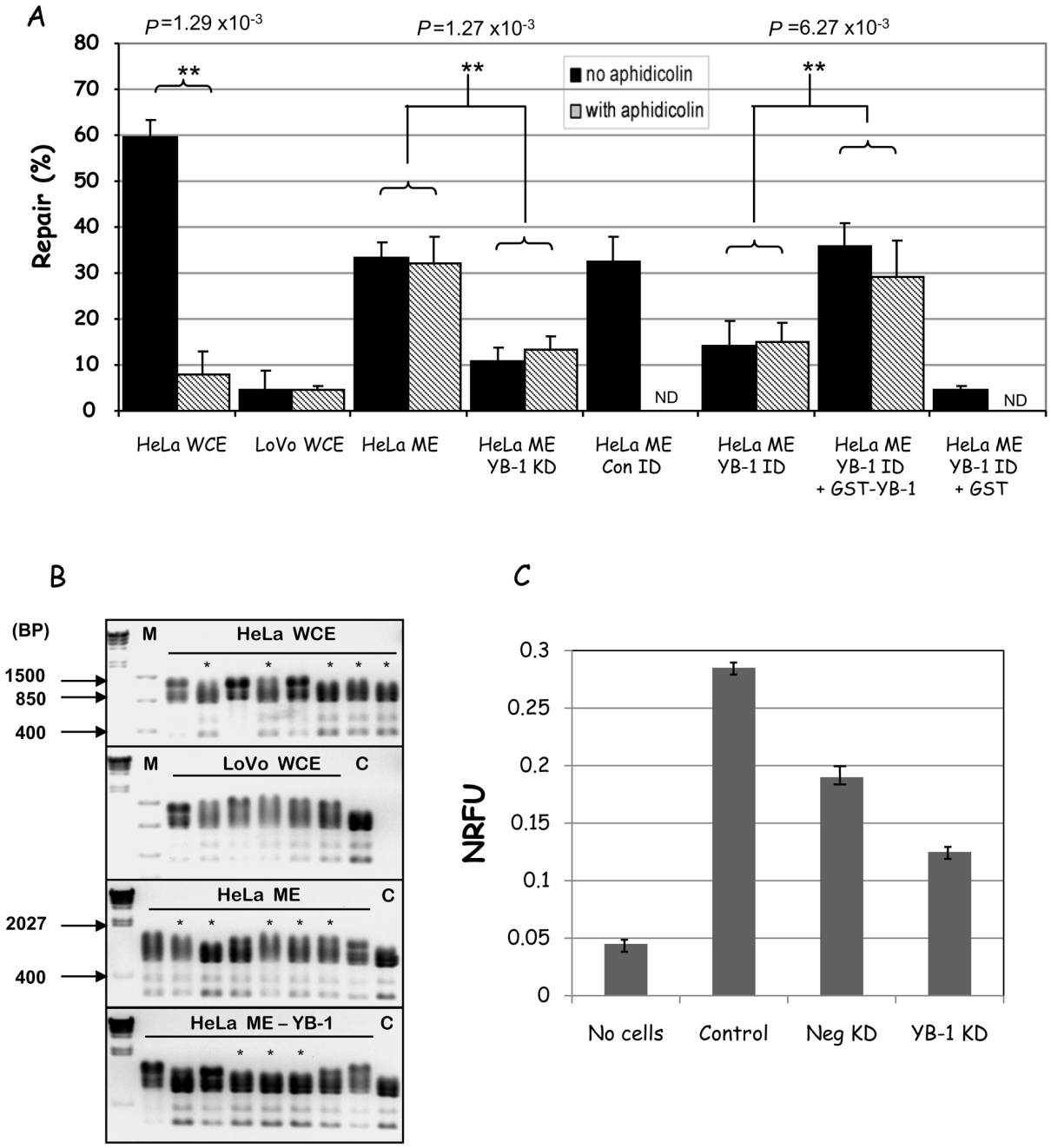

Figure 7.

A. MMR activity measured using the M13 dG/dG mismatched substrate, as described before, in absence (black bars) or presence (striped bars) of aphidicolin. Where indicated, YB-1 deficient lysates were from the immunodepletion (ID) or knockdown (KD) as above. Repair data and significances are given as before. Differences were analysed using Student's *t*-test. ND = not determined. **B.** MMR activity measured using restriction digest analysis of dG/T mismatched substrates after *in vitro* incubation with the extracts. Repaired plasmids for each lysate are marked (*); repaired plasmids show 3 bands after *Tfi*1 digestion (865 bp, 793 bp, and 346 bp), while unrepaired show 4 bands after *Tfi*1 digestion (1139 bp, 865 bp, 793 bp, and 346 bp). Crude repair percentages were calculated as the fraction of repaired plasmids over the

NIH-PA Author Manuscript

NIH-PA Author Manuscript

NIH-PA Author Manuscript

total screened, e.g. for HeLa WCE has 5/8 repair = 63%. Lane 1 in each gel is Lambda ladder after *HindIII* digest and M = Fermentas FastRuler low range molecular weight marker; sizes are marked (BP = base pairs). C = digested (non-mismatched) plasmid control. **C**. Cellular oxygen consumption for HeLa cells mock-transfected (control) or transfected with scrambled (Neg KD) or YB-1 (YB-1 KD) siRNAs was measured using the BD Oxygen Biosensor System. Normalized relative fluorescence units (NRFU) were obtained by normalizing the values to 0% O_2 dissolved, after the addition of sodium borohydride. Lower NRFU indicate more O_2 dissolved in the medium and therefore lower oxygen consumption; a control with no cells in the wells is shown as reference. The values presented are the average ± STD of two independent experiments.

NIH-PA Author Manuscript

NIH-PA Author Manuscript

NIH-PA Author Manuscript

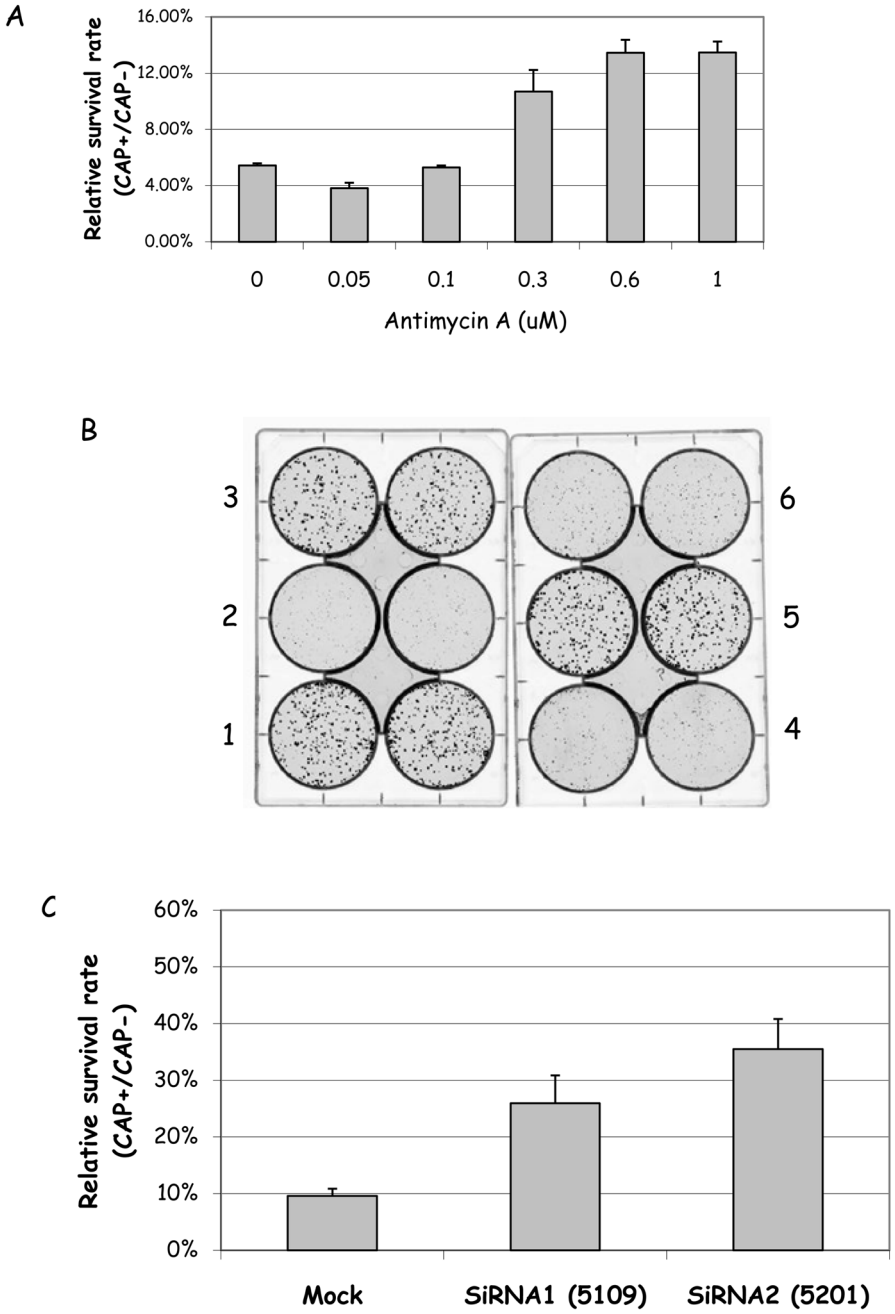

Figure 8.

A. HeLa cells were exposed to increasing concentrations of Antimycin A for 72 hrs; the cells were then replated at 500 cells/well and selected for CAP resistance in presence of 300 μg/ml of chloramphenicol. Resistant colonies were counted 7 days later. The results represent the average ± STD of two independent experiments, performed in triplicate. **B**. HeLa cells were either mock-transfected (1 and 2) or transfected with siRNAs against YB-1 (3–6), as described earlier. After 72 h the cells were replated at 500 cells/well and selected for CAP resistance, as above. After 7 days, the colonies were visualized and counted. This image is a representative of 3 independent experiments. Wells 1, 3 and 5 show cells mock-transfected or transfected with siRNA 1 and 2, respectively, grown in absence of CAP; wells 2, 4 and 6 show the same

cells, respectively, grown in presence of 300 300 μg/ml CAP. C. Quantification of the results obtained with mock- and YB-1 siRNA-transfected HeLa cells, selected for CAP-resistance as described above. The results presented are the average ± STD of two independent experiments, performed in duplicate.

NIH-PA Author Manuscript

NIH-PA Author Manuscript

NIH-PA Author Manuscript

NIH-PA Author Manuscript

NIH-PA Author Manuscript

NIH-PA Author Manuscript

Table 1

DNA substrates used in this study.

Name	Sequence	Structure
Control	5′-ATATACCGC^{G}CCGGCCGATCAAGCTTATT 3′-TATATGGCGC$_{C}$GGCCGGCTAGTTCGAATAA	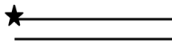
Mismatch	5′-ATATACCGC^{G}CCGGCCGATCAAGCTTATT 3′-TATATGGCGC$_{N}$GGCCGGCTAGTTCGAATAA	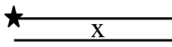
+ 1 IDL	5′-ATATACCGCGCCGGCCGATCAAGCTTATT 3′-TATATGGCGCCGGCCGGCTAGTTCGAATAA **C**	
+4 IDL	5′-ATATACCGCGCCGGCCGATCAAGCTTATT 3′-TATATGGCGCCGGCCGGCTAGTTCGAATAA **CG** **CG**	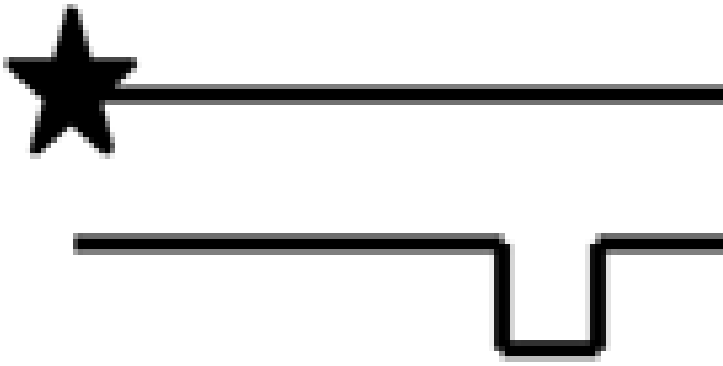
BrdU/MM	5′-ATATACCGC^{G}CCGGCCGATCAAGCTTATT-**BrU** 3′-TATATGGCGC$_{N}$GGCCGGCTAGTTCGAATAA	

NIH-PA Author Manuscript

NIH-PA Author Manuscript

NIH-PA Author Manuscript

Table 2

Quantification of binding on different substrates

Substrate	Binding (%)*
G/T	17.5 ± 3.4
+4 IDL	27.0 ± 7.0
+1 IDL	34.6 ± 6.8
G:C (Control)	9.1 ± 3.1

*Values are mean ± standard error from three independent experiments, expressed as the percentage reduction of total binding of mitochondrial substrates challenged with mismatched competitor DNA.

NIH-PA Author Manuscript

NIH-PA Author Manuscript

NIH-PA Author Manuscript

Table 3

Competition assay

Substrate	Reduction in Binding (%)*
G/G	71.4 ± 2.9
G/A	60.2 ± 0.7
G/T	60.6 ± 1.1
G:C (Control)	28.4 ± 2.8

*Values are mean ± standard error from three independent experiments, expressed as the percentage total shifted substrate.

NIH-PA Author Manuscript NIH-PA Author Manuscript NIH-PA Author Manuscript

Table 4

Top five binding candidates drawn from consensus data from eight separate affinity experiments (and multiple bands) and five EMSAs.

Protein	Size (kDa)	Acession #	Hits	EMSA	Affinity	Band Size	Mito
•Leucin-rich PPR motif containing proteins	130	54887383	5	Y	Y	110	Y
•Nuclease sensitive element binding protein 1 (human) Y-box binding protein 1	36	34098946	3	Y	N	—	N
•UV radiation resistance associated gene (human)	63	40674413	2	Y	N	—	N
•Human p32	32	4930075	4	Y	Y	80	Y
•Human mitochondrial single-stranded DNA binding protein	15 (56)	50513441		Y	Y	80, 50	Y

The number of times a particular protein was detected by MS analysis is shown, as well as whether it was from the affinity purification (in which case the band size it derived from is given) and/or from EMSA. The last column shows known mitochondrial localization ('Mito').

NIH-PA Author Manuscript

NIH-PA Author Manuscript

NIH-PA Author Manuscript

Table 5

M13 assay plaques counted

Sample	Plaques/no EtBr	Plaques/EtBr	Total plaques
Mock Moc	497	274	771
HeLa (positive control)	229	75	304
LoVo LoV (negative control)	147	98	245
HeLa mitoplasts	101	66	167
Sample	Plaques/no aphidicolin	Plaques/aphidicolin	Total plaques
Mock	1721	641	2362
HeLa (positive control)	1515	346	1861
LoVo (negative control)	1003	442	1445
HeLa mitoplasts	650	416	1066
HeLa mitoplasts with YB -1 knockdown	604	389	993
HeLa mitoplasts with immunodepletion control (IgG)	743	403	1146
HeLa mitoplasts with immunodepletion of YB-1	298	250	548
HeLa mitoplasts with immunodepletion of YB-1 and replacement GST -YB -1	810	382	1192
HeLa mitoplasts with immunodepletion of YB-1 and replacement GST	454	ND	454